

Discrete transparent boundary conditions for the Schrödinger equation: Fast calculation, approximation, and stability

Anton Arnold¹, Matthias Ehrhardt², Ivan Sofronov³

anton.arnold@math.uni-muenster.de,
ehrhhardt@math.tu-berlin.de, sofronov@spp.keldysh.ru

¹ Institut für Numerische Mathematik, Universität Münster, Einsteinstr. 62, D-48149 Münster, Germany

² Institut für Mathematik, Technische Universität Berlin, Str. des 17. Juni 136, D-10623 Berlin, Germany

³ Keldysh Institute of Applied Mathematics, Russian Academy of Sciences, Miusskaya sq. 4, Moscow, Russia

AMS 2000 Subject Classification: 65M12, 35Q40, 45K05

Key words: Schrödinger equation, transparent boundary conditions, discrete convolution, sum of exponentials, Padé approximations, finite difference schemes

December 6, 2002

Abstract

This paper is concerned with transparent boundary conditions (TBCs) for the time-dependent Schrödinger equation in one and two dimensions. Discrete TBCs are introduced in the numerical simulations of whole space problems in order to reduce the computational domain to a finite region. Since the discrete TBC for the Schrödinger equation includes a convolution w.r.t. time with a weakly decaying kernel, its numerical evaluation becomes very costly for large-time simulations.

As a remedy we construct approximate TBCs with a kernel having the form of a finite sum-of-exponentials, which can be evaluated in a very efficient recursion. We prove stability of the resulting initial-boundary value scheme, give error estimates for the considered approximation of the boundary condition, and illustrate the efficiency of the proposed method on several examples.

Acknowledgement

The first two authors were partially supported by the grants ERBFMRXCT-970157 (TMR–Network) from the EU and the DFG under Grant-No. AR 277/3-1. The second author was supported by the DFG research center Berlin “mathematics for key technologies”. The third author was partially supported by RFBR-Grant No. 01-01-00520 and by Saarland University. The authors acknowledge very stimulating discussions with Christian Lubich and Achim Schädle.

1 Introduction

The development of grid algorithms for solving initial–boundary–value problems on unbounded domains involves the question of formulating boundary conditions on an (artificial) boundary that cuts off a finite computational domain from the original, infinite portion of space. These boundary conditions (BCs) are not contained in the original problem formulation: they should be obtained by a transformation of the given asymptotic conditions at infinity onto the artificial boundary. Such a transfer must provide an approximation of the solution on the unbounded domain by the solution calculated in a finite domain with an artificial boundary. If the approximation is exact, the transfer is called *exact*, and the corresponding artificial boundary condition is called *exact* or *transparent*. For instance, different transparent boundary conditions (TBCs) for the *wave equation* are derived in [43, 40, 18, 41]; examples for other evolution problems are contained in [19].

Clearly, transparent boundary conditions permit us to consider computational domains of a minimal size, and therefore, they allow potentially to construct fast algorithms of computing solutions. However, there are several problems towards this goal: the first one is connected with the derivation of the boundary conditions themselves. Secondly, the numerical treatment (approximation, stability, efficiency) of corresponding analytical formulas for the BCs is a very delicate question. As a promising approach one can consider so–called *discrete transparent boundary conditions* (DTBCs) that are derived for a finite–difference approximation of the original evolution problem on an unbounded domain. The idea of such boundary conditions for general evolution difference equations is discussed in [32, 33]. DTBCs keep the approximation and stability properties of the difference scheme used. However,

usually there still remains the question of relatively high computational costs required for their implementation.

This paper is concerned with the numerical treatment of DTBCs for a finite–difference scheme of the 2D–Schrödinger equation governing the time evolution of the wave function $\psi(x, y, t) \in \mathbb{C}$ under the action of a given electrostatic potential $V(x, y, t) \in \mathbb{R}$.

Schrödinger equation. Consider a rectangular geometry that appears e.g. in the modeling of quantum waveguides and wave couplers (cf. [11]). In these applications the wave function $\psi(x, y, t)$ satisfies (within a good approximation) homogeneous Dirichlet BCs at the channel boundaries. Therefore, the (scaled) transient Schrödinger equation for such an (infinitely long) channel (or “lead”) of a waveguide reads:

$$\begin{aligned} i\psi_t &= -\frac{1}{2}\Delta\psi + V(x, y, t)\psi, & x \in \mathbb{R}, 0 < y < Y, t > 0, \\ \psi(x, 0, t) &= \psi(x, Y, t) = 0, \\ \psi(x, y, 0) &= \psi^I(x, y). \end{aligned} \tag{1.1}$$

We assume that the given potential V is constant outside of the *computational domain* $[0, X] \times [0, Y]$ (cf. Figure 1):

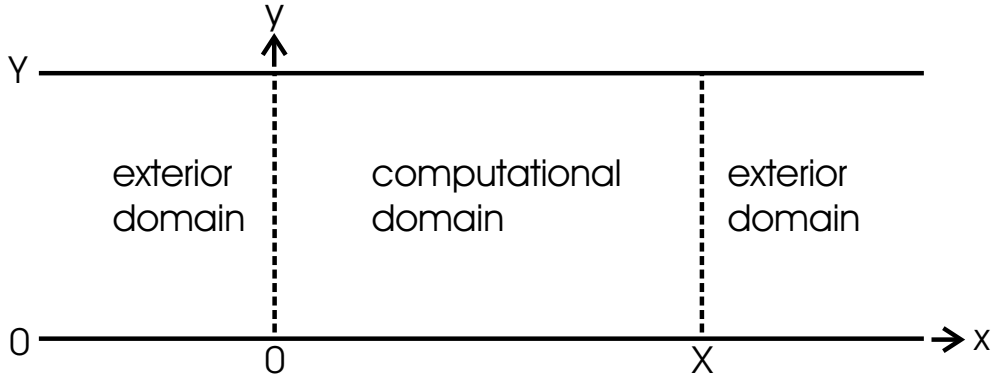


Figure 1: The artificial BCs at $x = 0$, $x = X$ cut off the exterior domains.

$$V(x, y, t) = V_- \equiv \text{const} \quad \text{for } x \leq 0, \quad V(x, y, t) = V_+ \equiv \text{const} \quad \text{for } x \geq X,$$

$0 < y < Y$, $t \geq 0$, and that the initial data has a compact support:

$$\text{supp } \psi^I \subset [0, X] \times [0, Y].$$

Discussions of strategies to soften these restrictions could be found in [22, 39, 6, 17].

Also, the computational domain is chosen here as a rectangle only for simplicity of the presentation. The geometry could be more complex, as it is the case in [11], e.g. The only constrains for our subsequent discussion of TBCs is that the exterior domains are semi-infinite strips (cf. [9] for a related stationary model).

Equation (1.1) has also important applications in optics (“*Fresnel equation*”, [37]) and acoustics (“*parabolic equation*”, [44]) as a paraxial approximation to the wave equation in the frequency domain.

Analytic TBCs. Let us exemplify first *analytic* TBCs that can be derived for the Schrödinger equation. For simplicity, we restrict us here to the 1D case when none of the considered functions depend on y . These TBCs were independently derived by several authors from various application fields (cf. [30, 8, 20]). They are non-local in t and read

$$\psi_x(0, t) = \sqrt{\frac{2}{\pi}} e^{-\frac{\pi}{4}i} \frac{d}{dt} \int_0^t \frac{\psi(0, \tau)}{\sqrt{t - \tau}} d\tau \quad (1.2)$$

for the left boundary at $x = 0$, and

$$\psi_x(X, t) = -\sqrt{\frac{2}{\pi}} e^{-\frac{\pi}{4}i} e^{-iV_+t} \frac{d}{dt} \int_0^t \frac{\psi(X, \tau) e^{iV_+\tau}}{\sqrt{t - \tau}} d\tau \quad (1.3)$$

for the right boundary at $x = X$.

Since TBCs are of memory-type, their numerical implementation requires to store the boundary data $\psi(0, \cdot)$ and $\psi(X, \cdot)$ of all the past history. Moreover, the discretization of the left and right TBCs (1.2), (1.3) is not trivial at all and has attracted lots of attention. For the many proposed strategies of discretizations of the TBCs (1.2), (1.3) (as well as semi-discrete approaches), we refer the reader to [3, 8, 10, 28, 35, 37] and references therein. We remark also that inadequate discretizations may introduce strong numerical reflections at the boundary or render the discrete initial boundary value problem only conditionally stable, see [17] for a detailed discussion.

Difference equations. We consider a Crank–Nicolson finite difference scheme, which is one of the commonly used discretization methods for the Schrödinger equation. With the uniform grid points $x_j = j\Delta x, y_k = k\Delta y$ (where $J\Delta x = X, K\Delta y = Y$), $t_n = n\Delta t$, and the approximation $\psi_{j,k,n} \sim \psi(x_j, y_k, t_n)$, $j \in \mathbb{Z}, 0 \leq k \leq K, n \in \mathbb{N}_0$, this scheme reads for the whole space problem:

$$\begin{aligned}
& -\frac{4i}{\Delta t}(\psi_{j,k,n+1} - \psi_{j,k,n}) \\
& = \frac{\psi_{j+1,k,n+1} - 2\psi_{j,k,n+1} + \psi_{j-1,k,n+1}}{\Delta x^2} + \frac{\psi_{j+1,k,n} - 2\psi_{j,k,n} + \psi_{j-1,k,n}}{\Delta x^2} \\
& + \frac{\psi_{j,k+1,n+1} - 2\psi_{j,k,n+1} + \psi_{j,k-1,n+1}}{\Delta y^2} + \frac{\psi_{j,k+1,n} - 2\psi_{j,k,n} + \psi_{j,k-1,n}}{\Delta y^2} \\
& - 2V_{j,k,n+\frac{1}{2}}(\psi_{j,k,n+1} + \psi_{j,k,n}), \quad j \in \mathbb{Z}, 1 \leq k \leq K-1, n \geq 0,
\end{aligned} \tag{1.4}$$

with

$$V_{j,k,n+\frac{1}{2}} = V(x_j, y_k, t_{n+\frac{1}{2}}).$$

Transparent boundary conditions are obtained by explicit solution of the equation in the two exterior domains $x \leq 0$ and $x \geq X$. In order to reduce the problem to the simpler 1D case, the Fourier method is used in y -direction. Due to the homogeneous Dirichlet BCs at the channel walls ($y = 0, y = Y$) we have

$$\psi_{j,0,n} = \psi_{j,K,n} = 0, \quad j \in \mathbb{Z}, n \geq 0, \tag{1.5}$$

and hence, use discrete Fourier transform of $\psi_{j,k,n}$ in y -direction with respect to sine-functions:

$$\psi_{j,n}^m := \frac{1}{K} \sum_{k=0}^{K-1} \psi_{j,k,n} \sin\left(\frac{\pi km}{K}\right), \quad m = 1, \dots, K-1.$$

The scheme (1.4), (1.5) in the two exterior domains $j \leq 0$ and $j \geq J$ then transforms into:

$$\begin{aligned}
& -\frac{4i}{\Delta t}(\psi_{j,n+1}^m - \psi_{j,n}^m) \\
& = \frac{\psi_{j+1,n+1}^m - 2\psi_{j,n+1}^m + \psi_{j-1,n+1}^m}{\Delta x^2} + \frac{\psi_{j+1,n}^m - 2\psi_{j,n}^m + \psi_{j-1,n}^m}{\Delta x^2} \\
& - 2V_j^m(\psi_{j,n+1}^m + \psi_{j,n}^m), \\
& V_j^m := V_j + \frac{1 - \cos \frac{\pi m}{K}}{\Delta y^2}, \quad j \in \mathbb{Z} \setminus [1, J-1], 1 \leq m \leq K-1, n \geq 0.
\end{aligned} \tag{1.6}$$

The modes ψ^m , $m = 1, \dots, K - 1$ are independent of each other in the exterior domains since the potential V is constant there. Therefore we can continue our analysis for a separate mode only.

Thus, by omitting the superscript m in the notation, we will consider a discrete 1D-Schrödinger equation of the following form:

$$\begin{aligned} -iR(\psi_{j,n+1} - \psi_{j,n}) &= \psi_{j+1,n+1} - 2\psi_{j,n+1} + \psi_{j-1,n+1} \\ &+ \psi_{j+1,n} - 2\psi_{j,n} + \psi_{j-1,n} - wV_{j,n+\frac{1}{2}}(\psi_{j,n+1} + \psi_{j,n}), \end{aligned} \quad (1.7)$$

where

$$R = \frac{4\Delta x^2}{\Delta t}, \quad w = 2\Delta x^2, \quad V_{j,n+\frac{1}{2}} = V(x_j, t_{n+\frac{1}{2}}),$$

$$V(x, t) = V_- \quad \text{for } x \leq 0, \quad V(x, t) = V_+ \quad \text{for } x \geq X, t \geq 0, \quad (1.8)$$

with constant V_- and V_+ . We remark that the spatial discretization on the computational interval $[0, X]$ can be nonuniform (*e.g. adaptive in time*) for our subsequent analysis.

Note two important advantages of this second order (in Δx and Δt) scheme: it is unconditionally stable, and it preserves the discrete L^2 -norm

$$\|\psi_n\|_2^2 := \Delta x \sum_{j \in \mathbb{Z}} |\psi_{j,n}|^2$$

with respect to time (these properties will be used for stability analysis in §5).

Discrete TBCs. Discrete transparent boundary conditions for the equation (1.7) were introduced in [4]. These DTBCs at the two boundary points $j = 0$ and $j = J$ (with $X = J\Delta x$) can most easily be expressed for the Z -transformed problem:

$$\hat{\psi}_1(z) = \hat{\ell}_0(z)\hat{\psi}_0(z), \quad \hat{\psi}_{J-1}(z) = \hat{\ell}_J(z)\hat{\psi}_J(z), \quad (1.9)$$

where the Z -transform of the sequence $\{\psi_{j,n}\}, n \in \mathbb{N}_0$ (with j considered fixed) is defined as the Laurent series, see [15]:

$$\mathcal{Z}\{\psi_{j,n}\} = \hat{\psi}_j(z) := \sum_{n=0}^{\infty} \psi_{j,n} z^{-n}, \quad z \in \mathbb{C}. \quad (1.10)$$

The two transformed boundary kernels $\hat{\ell}_j(z)$ are respectively calculated as (cf. [4, 17]):

$$\hat{\ell}_0(z) = 1 - i\zeta_0 \pm \sqrt{-\zeta_0(\zeta_0 + 2i)}, \quad \zeta_0 = \frac{Rz - 1}{2z + 1} + i\Delta x^2 V_-, \quad (1.11a)$$

$$\hat{\ell}_J(z) = 1 - i\zeta_J \pm \sqrt{-\zeta_J(\zeta_J + 2i)}, \quad \zeta_J = \frac{Rz - 1}{2z + 1} + i\Delta x^2 V_+. \quad (1.11b)$$

In order to have decaying solutions $\hat{\psi}_j(z)$ outside of the computational domain (i.e. for $j \rightarrow \pm\infty$) we have to choose the branch of the square root such that $|\hat{\ell}_0(z)| > 1$ and $|\hat{\ell}_J(z)| > 1$. The inverse \mathcal{Z} -transform of $\hat{\ell}_j$, $j = 0, J$ then defines the convolution coefficients for the DTBCs:

$$\{\ell_{j,n}\} := \mathcal{Z}^{-1}\{\hat{\ell}_j(z)\}, \quad j = 0, J.$$

Since the magnitude of $\ell_{j,n}$ does not decay as $n \rightarrow \infty$ ($\ell_{j,n}$ behaves like $\text{const} \cdot (-1)^n$ for large n), it is more convenient to use a modified formulation of the DTBCs (cf. [17]). We introduce

$$\hat{s}_j(z) := \frac{z + 1}{z} \hat{\ell}_j(z), \quad j = 0, J, \quad (1.12)$$

and

$$\{s_{j,n}\} = \mathcal{Z}^{-1}\{\hat{s}_j(z)\}, \quad (1.13)$$

which satisfy

$$s_{j,0} = \ell_{j,0}, \quad s_{j,n} = \ell_{j,n} + \ell_{j,n-1} = \mathcal{O}(n^{-\frac{3}{2}}), \quad n \geq 1. \quad (1.14)$$

The corresponding Laurent series of

$$\hat{s}_j(z) = \sum_{n=0}^{\infty} s_{j,n} z^{-n} \quad (1.15)$$

converges (and is continuous) for $|z| \geq 1$ because of the decay (1.14).

In physical space the DTBCs then read (cf. Th. 3.8 in [17]):

$$\psi_{1,n} - s_{0,0}\psi_{0,n} = \sum_{k=1}^{n-1} s_{0,n-k}\psi_{0,k} - \psi_{1,n-1}, \quad n \geq 1, \quad (1.16a)$$

$$\psi_{J-1,n} - s_{J,0}\psi_{J,n} = \sum_{k=1}^{n-1} s_{J,n-k}\psi_{J,k} - \psi_{J-1,n-1}, \quad n \geq 1, \quad (1.16b)$$

with the explicitly calculated convolution kernel:

$$s_{j,n} = \left[1 - i\frac{R}{2} + \frac{\sigma_j}{2}\right]\delta_{n,0} + \left[1 + i\frac{R}{2} + \frac{\sigma_j}{2}\right]\delta_{n,1} + \alpha_j e^{-in\varphi_j} \frac{P_n(\mu_j) - P_{n-2}(\mu_j)}{2n-1}, \quad (1.17)$$

$$\varphi_j = \arctan \frac{2R(\sigma_j + 2)}{R^2 - 4\sigma_j - \sigma_j^2}, \quad \mu_j = \frac{R^2 + 4\sigma_j + \sigma_j^2}{\sqrt{(R^2 + \sigma_j^2)[R^2 + (\sigma_j + 4)^2]}}$$

$$\sigma_j = 2\Delta x^2 V_j, \quad \alpha_j = \frac{i}{2} \sqrt{(R^2 + \sigma_j^2)[R^2 + (\sigma_j + 4)^2]} e^{i\varphi_j/2}, \quad j = 0, J.$$

Here P_n denotes the Legendre polynomials ($P_{-1} \equiv P_{-2} \equiv 0$), and $\delta_{n,k}$ is the Kronecker symbol. We have assumed that the initial condition satisfies $\psi_{0,0} = \psi_{1,0} = 0$ and $\psi_{J-1,0} = \psi_{J,0} = 0$.

The use of the formulas (1.16) for calculations permits us to avoid any boundary reflections and it renders the fully discrete scheme unconditionally stable (just like the underlying Crank–Nicolson scheme). However, the linearly in t increasing numerical effort to evaluate the DTBCs can sharply raise the total computational costs. Note that we need to evaluate just one convolution of (1.16) at each time step (at the endpoint of the interval $[0, t_n]$). Since the other points of this convolution are not needed, using an FFT is not practical. A strategy to overcome this drawback will be the key issue of this paper.

The considered DTBCs (1.16) include the discrete convolution of the unknown function with a given kernel (1.17). Our approach for fast evaluation of this convolution consists of approximating the kernel by a finite sum of exponentials that *decay* with respect to time (cf. [26]): this will permit us

to use recurrence formulas for the time stepping, see Section 4. Such kind of trick has been proposed in [40] for the continuous TBC in case of the 3D wave equation, and developed in [1, 2, 41, 42, 13, 19] for various hyperbolic problems.

Related results. As for the Schrödinger equation, we remark that a related approach was proposed by Bruneau and Di Menza ([10, 14]). There the authors consider the *continuous* TBC in Laplace space (for $V_- = 0$):

$$\hat{\psi}_x(0, s) = \sqrt{2}e^{-\frac{\pi}{4}i} \sqrt[4]{s} \hat{\psi}(0, s); \quad s = i\xi, \quad \xi \in \mathbb{R} \quad (1.18)$$

where $\sqrt[4]{\cdot}$ denotes the branch of the square root with positive real part. Its symbol $\sqrt[4]{s}$ is represented by a rational function calculated with the help of a least-squares approximation on the imaginary axis. This approach gives decaying sums of exponentials for the convolution kernel but does not allow for a convergence analysis or error estimates of the resulting finite difference scheme (see Example 6.3 below).

The limit $\Delta x \rightarrow 0$ of the DTBCs (1.16) coincides with the temporally semi-discrete TBC of Schmidt and Deuffhard [37] and of Lubich and Schädle, cf. [25, 34]. On the other hand, alternative derivations of the DTBC (1.16) could be done by applying the *Mikusiński operator approach*, cf. [38], or the *operational calculus*, cf. [25], to the convolution-type BC of the spatially semi-discretized Schrödinger equation. A temporal semi-discretization of the Dirichlet-to-Neumann map for the Schrödinger equation on a circular domain was discussed in [34, 35].

In [26, 36] the continuous convolution kernel of the TBC for the Schrödinger equation and its spatial semi-discretization is approximated by sums of exponentials $e^{\lambda_j t}$ including terms with $\operatorname{Re}(\lambda_j) > 0$, i.e. *not decaying* with respect to time. However, the authors propose an algorithm allowing to maintain a uniform relative error of the convolution kernel, but it requires to introduce new sums of exponentials to handle time intervals of an exponentially growing length.

Notice that all of the key ideas that we use for the Schrödinger equation here can easily be generalized to parabolic problems where the DTBCs have a similar form, see [16], e.g.

The paper is organized as follows. In §2 we discuss the numerical computation of the convolution coefficients (via the inverse Z -transform), approximate them by a discrete sum of exponentials in §3, and present an efficient

recursion for evaluating these approximate DTBCs in §4. In §5 we analyze the stability of the resulting initial-boundary-value scheme, and derive error estimates for the resulting Schrödinger solution in §6. Finally, the numerical examples of §7 illustrate the efficiency of the proposed method.

2 Calculation of convolution coefficients

The convolution coefficients $s_{0,n}$, $s_{j,n}$ appearing in the DTBC (1.16) can be calculated by the explicit formulae (1.17) as well as by 3-term-recurrence formulae, see [17]. Let us describe another, more general method based on a *numerical calculation* of the inverse Z -transform, see [15]. According to the definition of the Z -transform, see (1.10), we need to calculate the coefficients of the Laurent series (1.15). By using the Cauchy integral representation on the circle with a radius $\rho > 1$ one obtains

$$s_n = \frac{\rho^n}{2\pi} \int_0^{2\pi} \hat{s}(\rho e^{i\varphi}) e^{in\varphi} d\varphi, \quad n \in \mathbb{N}_0, \quad (2.1)$$

(for simplicity of notation we suppress here the index j).

The numerical approximation of (2.1) is made by the standard N -point summation rule:

$$s_n \approx s_n^{(N)} = \frac{\rho^n}{N} \sum_{k=0}^{N-1} \hat{s}(\rho e^{i\varphi_k}) e^{in\varphi_k}, \quad n = 0, 1, \dots, N-1, \quad (2.2)$$

where $\varphi_k = 2\pi k/N$. It is easy to show that the sum (2.2) yields the first N values of s_n with the accuracy

$$s_n^{(N)} = s_n + \mathcal{O}(\rho^{-N}), \quad n = 0, 1, \dots, N-1, \quad (2.3)$$

provided that the sequence $\{s_n\}$ is bounded: Indeed, using the Laurent series (1.15) with $z = \rho e^{i\varphi}$ and taking into account the orthogonality property

$$\sum_{k=0}^{N-1} e^{in\varphi_k} e^{-im\varphi_k} = N\delta_{n,(m \bmod N)}$$

we obtain

$$s_n^{(N)} = \frac{\rho^n}{N} \sum_{k=0}^{N-1} e^{in\varphi_k} \left(\sum_{m=0}^{\infty} s_m \rho^{-m} e^{-im\varphi_k} \right) = s_n + \rho^{-N} s_{n+N} + \rho^{-2N} s_{n+2N} + \dots .$$

Hence

$$|s_n^{(N)} - s_n| \leq \frac{\rho^{-N}}{1 - \rho^{-N}} \max_{k \geq N} |s_k|, \quad n = 0, 1, \dots . \quad (2.4)$$

Estimate (2.4) means that we can obtain very accurate coefficients $s_n^{(N)}$ if we take an appropriate value of ρ greater than 1: supposing that $\max_{k \geq N} |s_k| < 1 - \rho^{-N}$, we find from (2.4) that the accuracy

$$\varepsilon := \max_{n \geq 0} |s_n^{(N)} - s_n|$$

can be guaranteed by the choice $\rho \geq \varepsilon^{-\frac{1}{N}}$; for example if $\varepsilon = 10^{-6}$, $N = 50$ then $\rho \geq 1.32$.

Note that estimates of kind (2.4) are well-known, see e.g. [24], [27], and references therein.

Remark. By using the asymptotic behaviour $|s_n| \leq Cn^{-3/2}$, see (1.14), we get the sharper estimate

$$\rho \geq \left(1 + \frac{C}{\varepsilon} N^{-3/2}\right)^{1/N}.$$

We shall now describe some numerical aspects of evaluating the inverse Z -transform. Our tests show that the numerical inverse Z -transformation based on (2.2) is very sensitive to the *mantissa length* (parameter **Digits** in Figure 2), i.e. to the round-off error. For large numbers N , e.g. $N > 100$, the usual accuracy (e.g. **Digits**=15) could be insufficient.

For instance, Figure 2 shows the relative error (discrete L^2 -norm) of $s_n^{(N)}$ in dependence of $\rho \geq 1$ using $N = 256$ integration points. The curves look like a ‘hook’: for each fixed mantissa length the error first drops with increasing ρ in accordance with the error estimate (2.4); for larger ρ it then grows because of exponential amplification of the round-off errors due to the factor ρ^N in (2.2). Note that for different values of **Digits** the decreasing

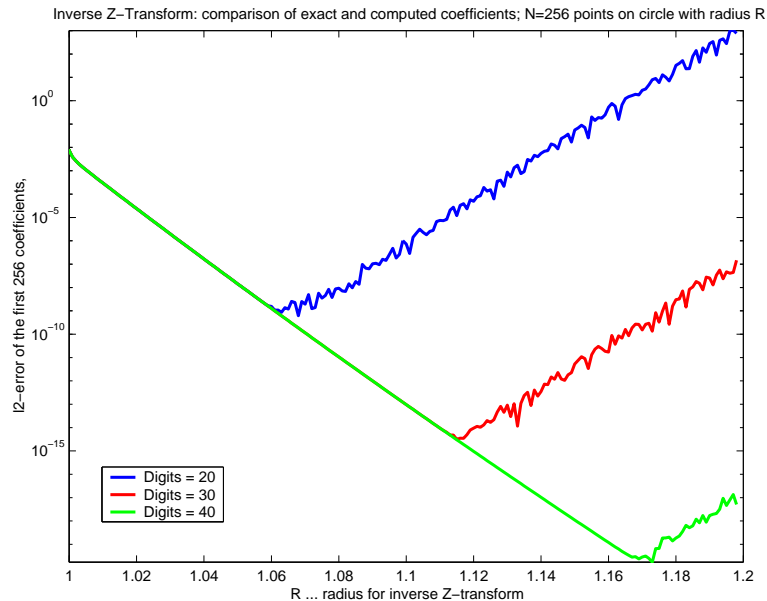


Figure 2: Relative error of the numerical inverse Z -transform of \hat{s} depending on ρ (the radius of the integration circle) for different values of **Digits** (the mantissa length). The three curves overlap exactly on the decaying branch, and their increasing branches – corresponding to the amplified round-off error – are 10 orders of magnitude apart. Here $\Delta x = 1/160$, $\Delta t = 2 \cdot 10^{-5}$, $N = 256$.

part of the error curve (corresponding to the approximation error) overlaps exactly. For further discussions of the numerical inverse Z -transform, we refer the reader to [24] where, in particular, the question of choosing the computational radius ρ in (2.2) is considered, and to [45] where a detailed numerical investigation of this situation is given.

3 Approximation of convolution coefficients by sums of exponentials

In order to derive a fast numerical method to calculate the discrete convolutions in (1.16) (for the algorithm cf. Section 4), we will approximate the

coefficients s_n by the following ansatz (sum of exponentials):

$$s_n \approx \tilde{s}_n := \begin{cases} s_n, & n = 0, \dots, \nu - 1, \\ \sum_{l=1}^L b_l q_l^{-n}, & n = \nu, \nu + 1, \dots, \end{cases} \quad (3.1)$$

where $L \in \mathbb{N}$, $\nu \geq 0$ are fixed numbers. Evidently, the approximation properties of \tilde{s}_n depend on L , ν , and the corresponding set $\{b_l, q_l\}$. Thus, the choice of an (in some sense) optimal such approximation is a difficult nonlinear problem. Below we propose a deterministic method of finding $\{b_l, q_l\}$ for fixed L and ν .

The ‘‘split’’ definition of $\{\tilde{s}_n\}$ in (3.1) is motivated by the fact that the implementation of the DTBCs (1.16) involves a convolution sum with k ranging only from 1 to $k = n - 1$. Since the first coefficient s_0 does not appear in this convolution, it makes no sense to include it in our sum-of-exponential approximation, which aims at simplifying the evaluation of the convolution. Hence, one may choose $\nu = 1$ in (3.1). The ‘‘special form’’ of s_0 and s_1 in definition (1.17) suggests even to exclude s_1 from this approximation and to choose $\nu = 2$ in (3.1); note that $\alpha^{-1} e^{in\varphi} s_n \in \mathbb{R}$ for $n \geq 2$. We use this choice in our numerical implementation.

Also, for the choice $\nu = 0$ (or $\nu = 1$) we typically obtain two (or one) coefficient pairs (b_l, q_l) of big magnitude. These ‘‘outlier’’ values reflect the different nature of the first two coefficients. Since the corresponding exponentials $b_0 q_0^{-n}$, $b_1 q_1^{-n}$ decay very quickly, they only yield a contribution in (3.1) for n very small.

Let us fix L and ν in (3.1), and consider the formal power series:

$$f(x) := s_\nu + s_{\nu+1}x + s_{\nu+2}x^2 + \dots \quad (3.2)$$

for $|x| \leq 1$. If there exists the $[L - 1|L]$ Padé approximation

$$\tilde{f}(x) := \frac{P_{L-1}(x)}{Q_L(x)} \quad (3.3)$$

of (3.2), then its Taylor series

$$\tilde{f}(x) = \tilde{s}_\nu + \tilde{s}_{\nu+1}x + \tilde{s}_{\nu+2}x^2 + \dots \quad (3.4)$$

satisfies the conditions

$$\tilde{s}_n = s_n, \quad n = \nu, \nu + 1, \dots, 2L + \nu - 1, \quad (3.5)$$

according to the definition of the Padé approximation rule.

Theorem 3.1. Let $Q_L(x)$ have L simple roots q_l with $|q_l| > 1$, $l = 1, \dots, L$. Then

$$\tilde{s}_n = \sum_{l=1}^L b_l q_l^{-n}, \quad n = \nu, \nu + 1, \dots, \quad (3.6)$$

where

$$b_l := -\frac{P_{L-1}(q_l)}{Q'_L(q_l)} q_l^{\nu-1} \neq 0, \quad l = 1, \dots, L. \quad (3.7)$$

Proof. We use the following known representation of the rational function (3.3):

$$\frac{P_{L-1}(x)}{Q_L(x)} = \sum_{l=1}^L \frac{b_l q_l^{1-\nu}}{q_l - x} \quad (3.8)$$

in terms of $\{b_l, q_l\}$ defined in the formulation of this theorem, see e.g. [13]. Substituting the identity

$$\frac{1}{q_l - x} = q_l^{-1} \sum_{n=0}^{\infty} \left(\frac{x}{q_l}\right)^n \quad (3.9)$$

(with $|x| < |q_l|$) in (3.8), we obtain (3.6) by comparing equations (3.3) and (3.4). \square

Remark. All our practical calculations confirm that the assumption on $Q_L(x)$ in Theorem 3.1 holds for any desired L , although we cannot prove this.

It follows from (3.5) and (3.6) that the set $\{b_l, q_l\}$ defined in Theorem 3.1 can be used in (3.1) at least for $n = \nu, \nu + 1, \dots, 2L + \nu - 1$. The main question now is: is it possible to use these $\{b_l, q_l\}$ also for $n > 2L + \nu - 1$? In other words, what quality of approximation

$$\tilde{s}_n \approx s_n, \quad n > 2L + \nu - 1 \quad (3.10)$$

can we expect?

Having in mind to outline our approach for a general case (not only for the specific s_n defined in (1.17)) we will use (a slight generalization of) the *Baker-Gammel-Wills conjecture* [7] concerning the existence of convergent subsequences of diagonal Padé approximants.

Conjecture (generalization of Baker-Gammel-Wills, [7]). *Let $p(x)$ be a power series representing a function which is meromorphic in $|x| < 1$ and continuous on $|x| \leq 1$ (except at the poles inside the unit circle). Then, at least a subsequence of the $[L|L]$ Padé approximants converges uniformly to $p(x)$ (as $L \rightarrow \infty$) in the domain formed by removing from the closed unit disk small open circles around the poles of p .*

Remark. The study of $[L - 1|L]$ Padé approximants can be reduced to the study of the $[L|L]$ case by simply considering Padé approximants to $g(x) = xp(x)$.

Coming back to our function $f(x)$ with s_n defined in (1.17), we note that it is analytic on $|x| < 1$ and continuous on $|x| \leq 1$. This follows from the analogous properties of $\hat{s}(z)$ for $|z| \geq 1$.

Theorem 3.2. *If the Conjecture holds, we then have:*

- (i) *at least a subsequence of the $[L - 1|L]$ (bounded) Padé approximants to (3.2) converge uniformly on the disk $|x| \leq 1$, as $L \rightarrow \infty$;*
- (ii) *all roots of $Q_L(x)$ (of the above subsequence) have absolute values greater than 1;*
- (iii) *$|s_n - \tilde{s}_n| = \mathcal{O}(n^{-\frac{3}{2}})$.*

Proof. The power series (3.2) with s_n defined in (1.17) is analytic on $|x| < 1$ and continuous for $|x| \leq 1$. Therefore we obtain conclusion (i) immediately from the conjecture. The property (ii) follows from (i) and (3.8). Finally, (iii) follows from (ii) and (3.6), which shows that $|\tilde{s}_n| \rightarrow 0$ exponentially, and from (1.14). \square

The above analysis permits us to give the following description of the approximation to the convolution coefficients (1.17) by the representation (3.1) if we use a $[L - 1|L]$ Padé approximant to (3.2): the first $2L + \nu - 1$ coefficients are reproduced exactly, see (3.5); however, the asymptotic behaviour of s_n and \tilde{s}_n (as $n \rightarrow \infty$) differs strongly (algebraic versus exponential decay). A typical graph of $|s_n - \tilde{s}_n|$ versus n for $L = 20$ is shown in Figure 3.

So far we discussed how to calculate and to approximate the DTBCs for one *fixed* discretization of the 1D-Schrödinger equation. However, a nice property of the considered approach consists of the following: once the approximate convolution coefficients $\{\tilde{s}_n\}$ are calculated for particular

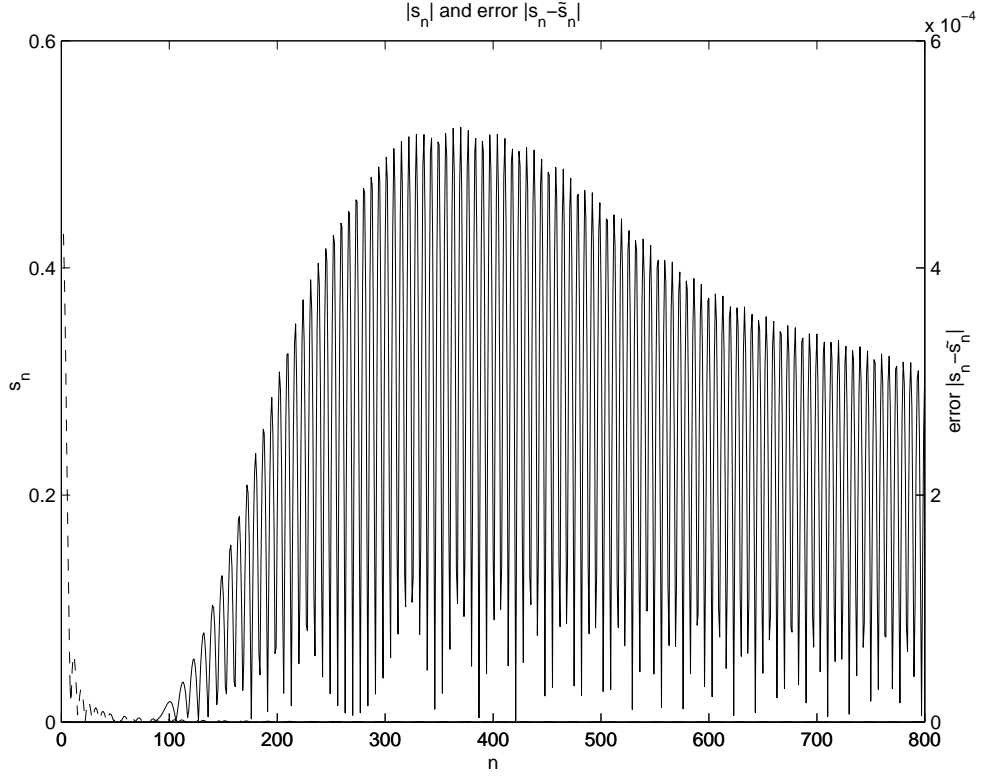


Figure 3: Convolution coefficients s_n (left axis, dashed line) and error $|s_n - \tilde{s}_n|$ of the convolution coefficients (right axis); $\Delta x = 1/160$, $\Delta t = 2 \cdot 10^{-5}$, $V = 0$ ($L = 20$)

discretization parameters $\{\Delta x, \Delta t, V\}$, it is easy to transform them into appropriate coefficients for any other discretization. We shall confine this discussion to the case $\nu = 2$:

Transformation rule 3.1. For $\nu = 2$, let the rational function

$$\hat{\tilde{s}}(z) = s_0 + \frac{s_1}{z} + \sum_{l=1}^L \frac{b_l}{q_l z - 1} \frac{1}{q_l z} \quad (3.11)$$

be the Z -transform of the convolution kernel $\{\tilde{s}_n\}_{n=0}^{\infty}$ from (3.1), where $\{\tilde{s}_n\}$ is assumed to be an approximation to a DTBC for the equation (1.7) with a given set $\{\Delta x, \Delta t, V\}$.

Then, for another set $\{\Delta x_*, \Delta t_*, V_*\}$, one can take the approximation

$$\hat{s}^*(z) := s_0^* + \frac{s_1^*}{z} + \sum_{l=1}^L \frac{b_l^*}{q_l^* z - 1} \frac{1}{q_l^* z}, \quad (3.12)$$

where

$$q_l^* := \frac{q_l \bar{a} - \bar{b}}{a - q_l \bar{b}}, \quad (3.13)$$

$$b_l^* := b_l q_l \frac{a \bar{a} - b \bar{b}}{(a - q_l \bar{b})(q_l \bar{a} - \bar{b})} \frac{1 + q_l^*}{1 + q_l}, \quad (3.14)$$

$$a := 2 \frac{\Delta x^2}{\Delta t} + 2 \frac{\Delta x_*^2}{\Delta t_*} + i(\Delta x^2 V - \Delta x_*^2 V_*), \quad (3.15)$$

$$b := 2 \frac{\Delta x^2}{\Delta t} - 2 \frac{\Delta x_*^2}{\Delta t_*} - i(\Delta x^2 V - \Delta x_*^2 V_*), \quad (3.16)$$

and s_0^* , s_1^* are the exact convolution coefficients for the parameters $\{\Delta x_*$, Δt_* , $V_*\}$ as given by (1.17).

Derivation. This transformation rule is based on the observation that the exact Z -transformed boundary kernel $\hat{\ell}(z) = \frac{z}{z+1} \hat{s}(z)$ depends on the parameters Δx , Δt , and V only via the variable

$$\zeta = 2 \frac{\Delta x^2}{\Delta t} \frac{z - 1}{z + 1} + i \Delta x^2 V, \quad (3.17)$$

cf. (1.11).

Making the assumption that also the *approximate* transformed boundary kernels

$$\hat{\tilde{\ell}}(z) := \frac{z}{z+1} \hat{s}(z), \quad (3.18)$$

$$\hat{\tilde{\ell}}^*(z^*) := \frac{z^*}{z^*+1} \hat{s}^*(z^*) \quad (3.19)$$

only depend on ζ yields a transformation between two sets of parameters (we shall elaborate on this choice in §5, cf. (5.12)). By equating the functions ζ and ζ^* corresponding to the sets $\{\Delta x, \Delta t, V\}$ and $\{\Delta x_*, \Delta t_*, V_*\}$, respectively, we obtain the map

$$z^* = \frac{az - b}{\bar{a} - \bar{b}z} \quad (3.20)$$

with a, b defined above.

With (3.18) and (3.19) the obvious transformation for $\hat{\ell}$, i.e.

$$\hat{\ell}^*(z^*) \equiv \hat{\ell}(z(z^*)) \quad \text{with } z(z^*) = \frac{\bar{a}z^* + b}{a + \bar{b}z^*}$$

translates into a transformation for \hat{s} :

$$\hat{s}^*(z^*) = \frac{z^* + 1}{z^*} \hat{\ell}^*(z^*) = \frac{z^* + 1}{z^*} \hat{\ell}(z(z^*)) = \frac{z^* + 1}{z^*} \frac{z(z^*)}{z(z^*) + 1} \hat{s}(z(z^*)). \quad (3.21)$$

Using $z(z^*)$ in (3.11) a lengthy but straight forward calculation yields

$$\hat{s}^*(z^*) = c_0^* + \frac{c_1^*}{z^*} + \sum_{l=1}^L \frac{b_l^*}{q_l^* z^* - 1} \frac{1}{q_l^* z^*}, \quad (3.22)$$

where q_l^* and b_l^* are defined, respectively, in (3.13) and (3.14). The constants c_0^* and c_1^* depend on $s_0, s_1, b_l,$ and q_l , and, in general, they do *not* coincide with the exact values s_0^* and s_1^* . For our purposes, however, this does not matter: Here, we are only interested in the transformation of the exponential approximation, since only this part enters the convolution (1.16) (cf. §4 below). And, otherwise, the calculation of $\{\tilde{s}_n\}$ would require to use the Padé-algorithm discussed in Theorem 3.1.

(3.22) shows that the transformation (3.21) preserves the structure of our approximate convolution coefficients $\{\tilde{s}_n\}$ as a sum of discrete exponentials for $n \geq \nu = 2$ (cf. (3.1)).

It remains to note that due to $|b| < |a|$, the *bilinear* function (3.20) maps the unit disc onto itself (see [21], e.g.). Therefore, for $|q_l| > 1$ the map (3.13) gives also $|q_l^*| > 1$. Hence, $\{\tilde{s}_n^*\}$ also contains only decaying exponentials. \square

We now return to the discrete 2D-Schrödinger equation, which was decomposed into the modes ψ^m , $m = 1, \dots, K - 1$ in (1.6). Provided an exponential approximation of DTBCs for a single mode is known, we can use formulas (3.13), (3.14) for a rapid calculation of approximate DTBCs for the remaining Fourier modes by taking the corresponding values V_j^m .

Example 3.1. (*Transformation rule*) We present a numerical example for applying the above transformation rule. For $L = 10$ we calculated the

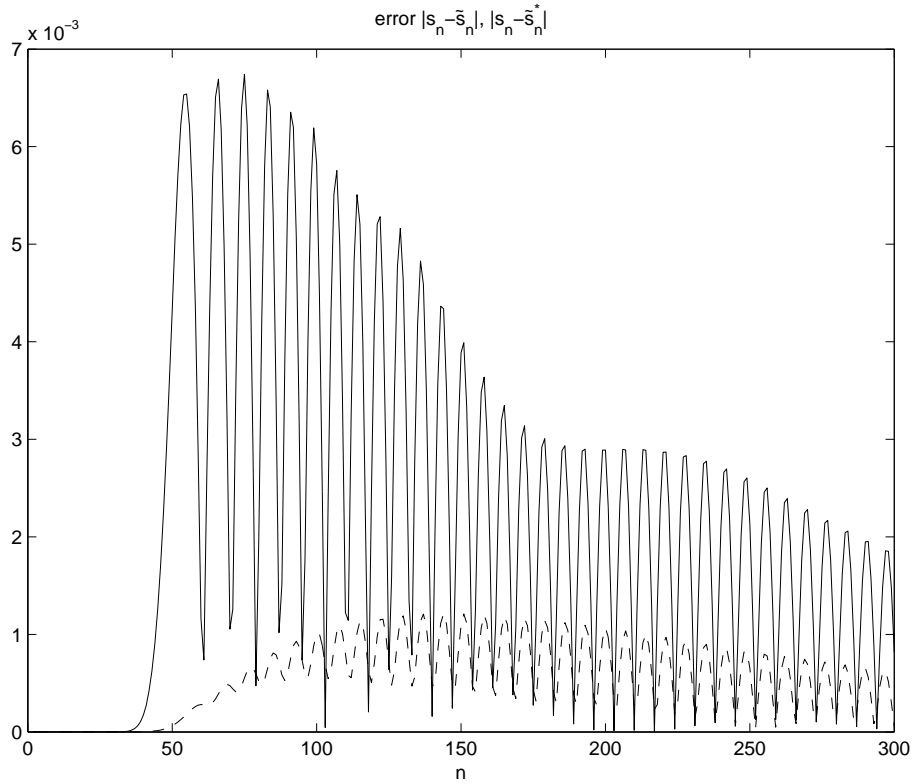


Figure 4: Approximation error of the approximate convolution coefficients for $\nu = 2$, $\Delta x = 1/160$, $\Delta t = 2 \cdot 10^{-5}$, $V = 4500$: The error of \tilde{s}_n^* (---) obtained from the transformation rule and the error of \tilde{s}_n (—) obtained from a direct Padé approximation of the exact coefficients s_n .

coefficients $\{b_l, q_l\}$ with the parameters $\Delta x = 1$, $\Delta t = 1$, $V = 0$ (cf. Appendix A) and then used the Transformation 3.1 to calculate the coefficients $\{b_l^*, q_l^*\}$ for the parameters $\Delta x_* = 1/160$, $\Delta t_* = 2 \cdot 10^{-5}$, $V_* = 4500$.

Figure 4 shows that the resulting convolution coefficients \tilde{s}_n^* are in this example even better approximations to the exact coefficients s_n than the coefficients \tilde{s}_n , which are obtained directly from the Padé algorithm discussed in Theorem 3.1. Hence, the numerical solution of the corresponding Schrödinger equation is also more accurate (cf. Example 7.2, Figure 17)

4 Fast evaluation of the discrete convolution with an “exponential” kernel

Let us consider the approximation (3.1) of the discrete convolution kernel appearing in the DTBC (1.16). With these “exponential” coefficients the convolution

$$C^{(n)}(u) := \sum_{k=1}^{n-\nu} u_k \tilde{s}_{n-k}, \quad \tilde{s}_n = \sum_{l=1}^L b_l q_l^{-n}, \quad |q_l| > 1, \quad (4.1)$$

of a discrete function u_k , $k = 1, 2, \dots$, can be calculated by recurrence formulas. And this will reduce the numerical effort drastically (cf. Figure 18 in Example 7.2).

Theorem 4.1. *The function $C^{(n)}(u)$ from (4.1) for $n \geq \nu + 1$ is represented by*

$$C^{(n)}(u) = \sum_{l=1}^L C_l^{(n)}(u), \quad (4.2)$$

where

$$\begin{aligned} C_l^{(n)}(u) &= q_l^{-1} C_l^{(n-1)}(u) + b_l q_l^{-\nu} u_{n-\nu}, \quad n = \nu + 1, \nu + 2, \dots \\ C_l^{(\nu)}(u) &\equiv 0. \end{aligned} \quad (4.3)$$

Proof. A straightforward calculation yields:

$$C^{(n)}(u) = \sum_{k=1}^{n-\nu} u_k \sum_{l=1}^L b_l q_l^{-(n-k)} = \sum_{l=1}^L C_l^{(n)}(u),$$

with

$$C_l^{(n)}(u) := \sum_{k=1}^{n-\nu} b_l q_l^{-(n-k)} u_k.$$

And for each $C_l^{(n)}(u)$ we have the recursion:

$$C_l^{(n)}(u) = q_l^{-1} \sum_{k=1}^{n-\nu-1} b_l q_l^{-(n-1-k)} u_k + b_l q_l^{-\nu} u_{n-\nu} = q_l^{-1} C_l^{(n-1)}(u) + b_l q_l^{-\nu} u_{n-\nu},$$

with

$$C_l^{(\nu)}(u) \equiv 0.$$

□

Finishing the algorithmic part of this study let us summarize the steps of the proposed method to evaluate approximate DTBCs:

- Step 1:** Prescribe L, ν (e.g. $\nu = 2$) in (3.1), take $\Delta x = \Delta t = 1, \rho \geq 1, N \geq 2L + 1$, and calculate by (1.17) or (2.2) the coefficients $s_n^{(N)}, n = \nu, \nu + 1, \dots, 2L + \nu - 1$.
- Step 2:** Use the $[L-1|L]$ -Padé algorithm for the series (3.4) with $\tilde{s}_n := s_n^{(N)}, n = \nu, \nu + 1, \dots, 2L + \nu - 1$ in order to find $\{b_l, q_l\}$ for (3.1) in accordance with Theorem 3.1.
- The Steps 1 and 2 are made once and for all; see Appendix A with the table of coefficients for $L = 5, 10$.
- Step 3:** For given $\{\Delta x_*, \Delta t_*, V_*\}$ use formulas (3.13)-(3.16) with $\{\Delta x = 1, \Delta t = 1, V = 0\}$ and $\{b_l, q_l\}$ from Step 2 for the calculation of $\{b_l^*, q_l^*\}$.
- Step 4:** Implement the recurrence formulas (4.2), (4.3) to calculate approximate convolutions in (1.16). The coefficients $s_0^*, s_1^*, \dots, s_{\nu-1}^*$ have to be calculated by (1.17) or (2.2).

5 Stability analysis of the numerical scheme

In this section we shall give a stability analysis of our numerical scheme for the Schrödinger equation (1.7) along with BCs of convolution form like (1.16). Usually, these BCs will be exactly or approximatively transparent, depending on the chosen convolution kernel.

L²-a-priori estimate of continuous solution. To illustrate our subsequent calculations for the discrete case we shall first give an a-priori estimate for a continuous IBVP for the Schrödinger equation:

$$\begin{cases} i\psi_t &= -\frac{1}{2}\psi_{xx} + V(x, t)\psi, & 0 < x < X, t > 0, \\ \psi(x, 0) &= \psi^I(x), & 0 < x < X, \\ \psi_x(0, t) &= \int_0^t f_0(t - \tau)\psi(0, \tau) d\tau, & t > 0, \\ \psi_x(X, t) &= \int_0^t f_X(t - \tau)\psi(X, \tau) d\tau, & t > 0, \end{cases} \quad (5.1)$$

where $f_0(t)$, $f_X(t)$ are given functions.

Alternatively, the two boundary conditions can be written in the Laplace transform space as

$$\hat{\psi}_x(0, s) = \hat{f}_0(s)\hat{\psi}(0, s), \quad \operatorname{Re} s \geq 0, \quad (5.2a)$$

$$\hat{\psi}_x(X, s) = \hat{f}_X(s)\hat{\psi}(X, s), \quad \operatorname{Re} s \geq 0, \quad (5.2b)$$

where $\hat{f}_0(s)$ and $\hat{f}_X(s)$, $s \in \mathbb{C}$ are the Laplace transforms of $f_0(t)$ and $f_X(t)$, $t \geq 0$, respectively.

For the system (5.1) we have the following estimate:

Proposition 5.1. (Stability condition) *Let the transformed boundary kernels \hat{f}_0 , \hat{f}_X satisfy for some $\alpha_1 \in \mathbb{R}$:*

$$\operatorname{Im} \hat{f}_0(\alpha_1 + i\xi) \leq 0, \quad \operatorname{Im} \hat{f}_X(\alpha_1 + i\xi) \geq 0, \quad \forall \xi \in \mathbb{R}. \quad (5.3)$$

Then the solution of (5.1) satisfies the a-priori estimate

$$\|\psi(\cdot, t)\|_{L^2(0, X)} \leq \|\psi^I\|_{L^2(0, X)} e^{\alpha_1 t}, \quad t > 0. \quad (5.4)$$

Proof. For smooth solutions ψ this proposition is easily proved by using an energy estimate for the function $\phi(x, t) := \psi(x, t)e^{-\alpha_1 t}$ and by using Plancherel's identity for Laplace transforms:

$$\begin{aligned} \|\phi(\cdot, t)\|_{L^2(0, X)}^2 &\leq \|\psi^I\|_{L^2(0, X)}^2 + \operatorname{Im} \int_0^t [\phi(X, \tau) \overline{\phi_x(X, \tau)} - \phi(0, \tau) \overline{\phi_x(0, \tau)}] d\tau \\ &= \|\psi^I\|_{L^2(0, X)}^2 + \operatorname{Im} \int_0^\infty \left[\chi_{[0, t]}(\tau) \phi(X, \tau) \overline{\{(\chi_{[0, t]}\phi) * \tilde{f}_X\}(X, \tau)} \right. \\ &\quad \left. - \chi_{[0, t]}(\tau) \phi(0, \tau) \overline{\{(\chi_{[0, t]}\phi) * \tilde{f}_0\}(0, \tau)} \right] d\tau \\ &= \|\psi^I\|_{L^2(0, X)}^2 - \frac{1}{2\pi} \int_{\mathbb{R}} \left[|\widehat{\chi_{[0, t]}\phi}|^2(X, i\xi) \operatorname{Im} \hat{f}_X(\alpha_1 + i\xi) \right. \\ &\quad \left. - |\widehat{\chi_{[0, t]}\phi}|^2(0, i\xi) \operatorname{Im} \hat{f}_0(\alpha_1 + i\xi) \right] d\xi \\ &\leq \|\psi^I\|_{L^2(0, X)}^2. \end{aligned} \quad (5.5)$$

Here χ denotes the characteristic function, and we used the fact that

$$\phi_x(\tau) = (\phi * \tilde{f}_0)(\tau) = ((\chi_{[0, t]}\phi) * \tilde{f}_0)(\tau), \quad \tau \leq t,$$

with the notation $\hat{f}_0(s) = \hat{f}_0(\alpha_1 + s)$ (and analogously for f_X).

We remark that the calculation in (5.5) is rigorous for $\psi(0, \cdot), \psi(X, \cdot) \in L^2_{loc}(\mathbb{R}_0^+)$ and $f_0, f_X \in L^1_{loc}(\mathbb{R}_0^+)$ ¹. \square

Example 5.1. (Stability of TBC) *The functions*

$$\hat{f}_0^{\text{TBC}}(s) = \sqrt{2} e^{-\frac{\pi}{4}i} \sqrt{s + iV_-}, \quad \hat{f}_X^{\text{TBC}}(s) = -\sqrt{2} e^{-\frac{\pi}{4}i} \sqrt{s + iV_+} \quad (5.6)$$

correspond to the TBCs (1.2), (1.3). An easy calculation shows that they satisfy the stability conditions (5.3) for all $\alpha_1 \geq 0$.

However, the above regularity assumptions on $f_0^{\text{TBC}}, f_X^{\text{TBC}}$ are not satisfied here: With $V_- = 0$ the left TBC (1.2) reads

$$\psi_x(0, t) = \sqrt{2} e^{-\frac{\pi}{4}i} \frac{d^{\frac{1}{2}}\psi}{dt^{\frac{1}{2}}}(0, t),$$

where $\frac{d^{\frac{1}{2}}}{dt^{\frac{1}{2}}}$ denotes the semiderivative (cf. §7 in [29]). For smooth functions $\psi(0, \cdot)$ it can be rewritten as

$$\psi_x(0, t) = \sqrt{\frac{2}{\pi}} e^{-\frac{\pi}{4}i} \left[\frac{1}{2} \int_0^t \frac{\psi(0, t) - \psi(0, \tau)}{(t - \tau)^{3/2}} d\tau + \frac{\psi(0, t)}{\sqrt{t}} \right].$$

Apart of a singular (distributional) contribution at $t = 0$, its convolution kernel (as appearing in (5.1)) is

$$f_0^{\text{TBC}}(t) = -(2\pi)^{-\frac{1}{2}} e^{-\frac{\pi}{4}i} t^{-\frac{3}{2}}, \quad t > 0. \quad (5.7)$$

Note that this is the same decay rate as in the discrete case (1.14).

Obviously $f_0^{\text{TBC}} \notin L^1_{loc}(\mathbb{R}_0^+)$, but using higher regularity of ψ one can still give a sense to the boundary terms in (5.5): For a smooth potential V and for $\psi^I \in H^1(0, X)$ the solution of the Schrödinger equation has the regularity $\psi \in C([0, \infty), H^1(0, X))$ and its boundary traces satisfy $\psi(0, \cdot), \psi(X, \cdot) \in H^{\frac{1}{4}}_{loc}(\mathbb{R}_0^+)$ (cf. Chap. XVIII §1, §7 in [12] for details).

Using a zero-extension of some $\phi \in H^{\frac{1}{4}}(0, T)$ to $H^{\frac{1}{4}}(\mathbb{R}^+)$ and Plancherel's identity for Laplace transforms one easily verifies that $\frac{d^{\frac{1}{2}}\phi}{dt^{\frac{1}{2}}}$ is a continuous linear functional on $H^{\frac{1}{4}}(\mathbb{R}^+)$. And hence, the r.h.s. of (5.5) is well defined.

¹With L^p_{loc} we denote spaces of locally integrable functions.

where $\hat{g}_0(z)$, $\hat{g}_J(z)$ are given functions. Alternatively, the two BCs can be written as

$$\Delta^+ \psi_{0,n} = \psi_{0,n} * \tilde{g}_{0,n} = \sum_{k=0}^n \psi_{0,k} \tilde{g}_{0,n-k}; \quad \tilde{g}_{0,n} := g_{0,n} - \delta_{0,n}, \quad (5.11a)$$

$$\Delta^- \psi_{J,n} = -\psi_{J,n} * \tilde{g}_{J,n} = -\sum_{k=0}^n \psi_{J,k} \tilde{g}_{J,n-k}; \quad \tilde{g}_{J,n} := g_{J,n} - \delta_{0,n}. \quad (5.11b)$$

We assume that the Z -transforms of the given sequences $\{g_{j,n}\}$; $j = 0, J$, $\hat{g}_j(z) := \mathcal{Z}\{g_{j,n}\}$ are analytic in a neighbourhood of $z = \infty$.

Typically, the BCs (5.11) should be a discrete approximation of the two continuous, convolution-BCs in (5.1). And hence the two functions \hat{g}_j ; $j = 0, J$ are of course functions of z , Δx , and Δt , just as in the DTBCs (1.11a), (1.11b). In this example their functional dependence is of the form

$$\hat{\ell}_j \equiv \hat{g}_j(z, \Delta x, \Delta t) = \hat{h}_j(y) \quad \text{with } y = y(z, \Delta x, \Delta t) = \frac{R}{2} \left(\frac{z-1}{z+1} + i\nu_j \right), \quad (5.12)$$

where $\nu_j = \Delta t V_j / 2$ depends on the external potentials V_0 and V_J . In analogy to (1.8) we assume $V_j = V_-$ for $j \leq 0$ and $V_j = V_+$ for $j \geq J$. Note that y appearing in these discrete BCs is just the symbol of $\partial_t + iV$ in the Crank-Nicolson scheme, and the Z -transformed equation (1.7) can be recast in the exterior domain (i.e. for $j \leq 0$ or $j \geq J$) as

$$iy \hat{\psi}_j(z) = -\frac{\Delta^2}{2} \hat{\psi}_j(z).$$

Next we shall specify the typical Δx - and Δt -dependence of general transformed boundary kernels \hat{g}_j . For arbitrary functions f_0, f_x the BCs in (5.1) are usually *not* perfectly transparent. Therefore, their natural discretization cannot be obtained by calculating the discrete Dirichlet-to-Neumann map for the fully discretized whole space problem, as it was done in [4, 17] to derive the DTBCs.

After replacing ψ_x in the BCs (5.1) by a finite difference quotient we now discuss the time discretization of their convolution integrals: A very natural method is based on the *operational quadrature* of [23, 24] by using the same time discretization for the BCs as for the evolution equation, i.e. the

trapezoidal rule in our case. We shall hence assume that the transformed boundary kernels in (5.10) are also of the form

$$\hat{g}_j(z, \Delta x, \Delta t) = \hat{h}_j(y), \quad (5.13)$$

with y given in (5.12) and some appropriate function \hat{h}_j . We remark that this approach also reproduces the DTBCs (1.9)-(1.11b). In the Transformation rule 3.1 we had already assumed this form (5.13) when calculating the explicit Δx - and Δt -dependence of the sum-of-exponentials-BCs derived in §3.

ℓ^2 -a-priori estimate of discrete solution. In the following lemma we shall derive an a-priori estimate for the temporal growth of the solution to (5.10) with Δx and Δt considered fixed. This discrete analogue of Proposition 5.1 will then be the key ingredient for our stability result (given in Theorem 5.1 and Theorem 5.2 below). We shall use the discrete L^2 -norm:

$$\|\psi_n\|_2^2 := \Delta x \sum_{j=1}^{J-1} |\psi_{j,n}|^2. \quad (5.14)$$

Lemma 5.1. (Growth condition) *Let the transformed boundary kernels \hat{g}_0, \hat{g}_J satisfy*

$$\text{Im} \hat{g}_0(\beta e^{i\varphi}) \leq 0, \quad \text{Im} \hat{g}_J(\beta e^{i\varphi}) \leq 0, \quad \forall 0 \leq \varphi \leq 2\pi, \quad (5.15)$$

for some (sufficiently large) $\beta \geq 1$. Assume also that \hat{g}_0, \hat{g}_J are analytic for $|z| \geq \beta$. Then, the solution of (5.10) satisfies the a-priori estimate

$$\|\psi_n\|_2 \leq \|\psi_0\|_2 \beta^n, \quad n \in \mathbb{N}. \quad (5.16)$$

Proof. The proof is analogous to that of Proposition 5.1 and it is based on a discrete energy estimate for the new variable

$$\phi_{j,n} := \psi_{j,n} \beta^{-n},$$

which satisfies the equation

$$-iR(\phi_{j,n+1} - \phi_{j,n}) = \left(\Delta^2 - wV_{j,n+\frac{1}{2}} \right) (\phi_{j,n+1} + \phi_{j,n}) \quad (5.17a)$$

$$+ (\beta - 1) \left(\Delta^2 - wV_{j,n+\frac{1}{2}} + iR \right) \phi_{j,n+1}; \quad j = 1, \dots, J-1,$$

$$\phi_{j,0} = \psi_{j,0}; \quad j = 0, \dots, J, \quad (5.17b)$$

$$\Delta^+ \hat{\phi}_0(z) = (\hat{g}_0(\beta z) - 1) \hat{\phi}_0(z), \quad (5.17c)$$

$$\Delta^- \hat{\phi}_J(z) = -(\hat{g}_J(\beta z) - 1) \hat{\phi}_J(z). \quad (5.17d)$$

In physical space, the two BCs can be written as

$$\Delta^+ \phi_{0,n} = \phi_{0,n} * \frac{\tilde{g}_{0,n}}{\beta^n} = \sum_{k=0}^n \phi_{0,k} (\tilde{g}_{0,n-k} \beta^{k-n}), \quad (5.18a)$$

$$\Delta^- \phi_{J,n} = -\phi_{J,n} * \frac{\tilde{g}_{J,n}}{\beta^n} = -\sum_{k=0}^n \phi_{J,k} (\tilde{g}_{J,n-k} \beta^{k-n}). \quad (5.18b)$$

First we multiply (5.17a) by $\bar{\phi}_{j,n}/\beta$ and its complex conjugate by $\phi_{j,n+1}$:

$$\begin{aligned} -iR\bar{\phi}_{j,n}(\phi_{j,n+1} - \phi_{j,n}) &= \bar{\phi}_{j,n} \left(\Delta^2 - wV_{j,n+\frac{1}{2}} \right) (\phi_{j,n+1} + \phi_{j,n}) \quad (5.19) \\ &+ (\beta^{-1} - 1)\bar{\phi}_{j,n} \left(\Delta^2 - wV_{j,n+\frac{1}{2}} - iR \right) \phi_{j,n}, \end{aligned}$$

$$\begin{aligned} iR\phi_{j,n+1}(\bar{\phi}_{j,n+1} - \bar{\phi}_{j,n}) &= \phi_{j,n+1} \left(\Delta^2 - wV_{j,n+\frac{1}{2}} \right) (\bar{\phi}_{j,n+1} + \bar{\phi}_{j,n}) \quad (5.20) \\ &+ (\beta - 1)\phi_{j,n+1} \left(\Delta^2 - wV_{j,n+\frac{1}{2}} - iR \right) \bar{\phi}_{j,n+1}. \end{aligned}$$

Note that we used equation (5.17a) to modify the last term of (5.19). Next we subtract (5.20) from (5.19), sum from $j = 1$ to $j = J - 1$, and take imaginary parts. After a simple, but lengthy calculation we obtain:

$$\begin{aligned} \sum_{j=1}^{J-1} (|\phi_{j,n+1}|^2 - |\phi_{j,n}|^2) &= -(1 - \beta^{-1}) \sum_{j=1}^{J-1} |\phi_{j,n}|^2 - (\beta - 1) \sum_{j=1}^{J-1} |\phi_{j,n+1}|^2 \\ &+ \frac{1}{\beta R} \text{Im} \left[(\bar{\phi}_{0,n} + \beta\bar{\phi}_{0,n+1}) \Delta^+(\phi_{0,n} + \beta\phi_{0,n+1}) \right. \\ &\quad \left. - (\bar{\phi}_{J,n} + \beta\bar{\phi}_{J,n+1}) \Delta^-(\phi_{J,n} + \beta\phi_{J,n+1}) \right]. \quad (5.21) \end{aligned}$$

Summing (5.21) from $n = 0$ to $n = N$ yields (note that $\beta \geq 1$):

$$\begin{aligned} \|\phi_{N+1}\|_2^2 &\leq \|\phi_0\|_2^2 + \frac{\Delta x}{\beta^2 R} \text{Im} \sum_{n=0}^N \left[(\bar{\phi}_{0,n} + \beta\bar{\phi}_{0,n+1}) \Delta^+(\phi_{0,n} + \beta\phi_{0,n+1}) \right. \\ &\quad \left. - (\bar{\phi}_{J,n} + \beta\bar{\phi}_{J,n+1}) \Delta^-(\phi_{J,n} + \beta\phi_{J,n+1}) \right] \\ &= \|\phi_0\|_2^2 + \frac{\Delta x}{\beta^2 R} \text{Im} \sum_{n=0}^N \left[(\bar{\phi}_{0,n} + \beta\bar{\phi}_{0,n+1}) (\phi_{0,n} + \beta\phi_{0,n+1}) * \frac{\tilde{g}_{0,n}}{\beta^n} \right. \\ &\quad \left. + (\bar{\phi}_{J,n} + \beta\bar{\phi}_{J,n+1}) (\phi_{J,n} + \beta\phi_{J,n+1}) * \frac{\tilde{g}_{J,n}}{\beta^n} \right] \quad (5.22) \end{aligned}$$

For the last identity we used the BCs (5.18) and $\phi_{0,0} = \phi_{J,0} = 0$.

To finish the proof it remains to determine the sign of the last term in (5.22). To this end we define (for N fixed) the two sequences,

$$u_n := \begin{cases} \phi_{0,n} + \beta\phi_{0,n+1}, & n = 0, \dots, N, \\ 0, & n > N, \end{cases}$$

$$v_n := u_n * \frac{\tilde{g}_{0,n}}{\beta^n} = \sum_{k=0}^n u_k \frac{\tilde{g}_{0,n-k}}{\beta^{n-k}}, \quad n \in \mathbb{N}_0.$$

The Z -transform $\mathcal{Z}\{u_n\} = \hat{u}(z)$ is analytic for $|z| > 0$, since it is a finite sum. The Z -transform $\mathcal{Z}\{v_n\}$ then satisfies $\hat{v}(z) = (\hat{g}_0(\beta z) - 1)\hat{u}(z)$ and is analytic for $|z| \geq 1$. Using Plancherel's Theorem for Z -transforms (cf. §38 in [15]) we have

$$\begin{aligned} \sum_{n=0}^N v_n \bar{u}_n &= \sum_{n=0}^{\infty} v_n \bar{u}_n = \frac{1}{2\pi} \int_0^{2\pi} \hat{v}(e^{i\varphi}) \overline{\hat{u}(e^{i\varphi})} d\varphi \\ &= \frac{1}{2\pi} \int_0^{2\pi} |\hat{u}(e^{i\varphi})|^2 (\hat{g}_0(\beta e^{i\varphi}) - 1) d\varphi. \end{aligned} \quad (5.23)$$

Using (5.23) for the two boundary terms in (5.22) now gives:

$$\begin{aligned} \|\phi_{N+1}\|_2^2 &\leq \|\phi_0\|_2^2 + \frac{\Delta x}{2\pi\beta^2 R} \int_0^{2\pi} \left[|(1 + \beta e^{i\varphi})\hat{\phi}_0(e^{i\varphi})|^2 \operatorname{Im}(\hat{g}_0(\beta e^{i\varphi}) - 1) \right. \\ &\quad \left. + |(1 + \beta e^{i\varphi})\hat{\phi}_J(e^{i\varphi})|^2 \operatorname{Im}(\hat{g}_J(\beta e^{i\varphi}) - 1) \right] d\varphi. \end{aligned} \quad (5.24)$$

Our assumptions on \hat{g}_0 and \hat{g}_J hence imply

$$\|\phi_N\|_2 \leq \|\phi_0\|_2, \quad \forall N \geq 0,$$

and the result follows. \square

Remark. Above we have assumed that the two transformed boundary kernels \hat{g}_j ; $j = 0, J$ – as Z -transforms – are analytic for $|z| \geq \beta$. Hence their imaginary parts are harmonic functions there. Since the average of $\hat{g}_j(z)$ on the circles $z = \beta e^{i\varphi}$ equals $g_{j,0} = \hat{g}_j(z = \infty)$, condition (5.15) implies $\operatorname{Im} \hat{g}_j(z = \infty) \leq 0$; $j = 0, J$. Then we have the following simple consequence of the maximum principle for the Laplace equation:

If condition (5.15) holds for some β_0 , it also holds for all $\beta > \beta_0$.

Example 5.3. (Discrete counterpart of Example 5.1) For the exact DTBC (1.16) (with $\hat{g}_j = \hat{\ell}_j$, $j = 0, J$) the stability condition (5.15) is clearly satisfied for $\beta = 1$ (see Figure 5). In fact the DTBC satisfies (5.15) for all Δx and Δt . Hence, the discrete L^2 -norm of ψ_n always decreases monotonically in time. And in this case the L^2 -stability of the scheme (5.10) is trivial.

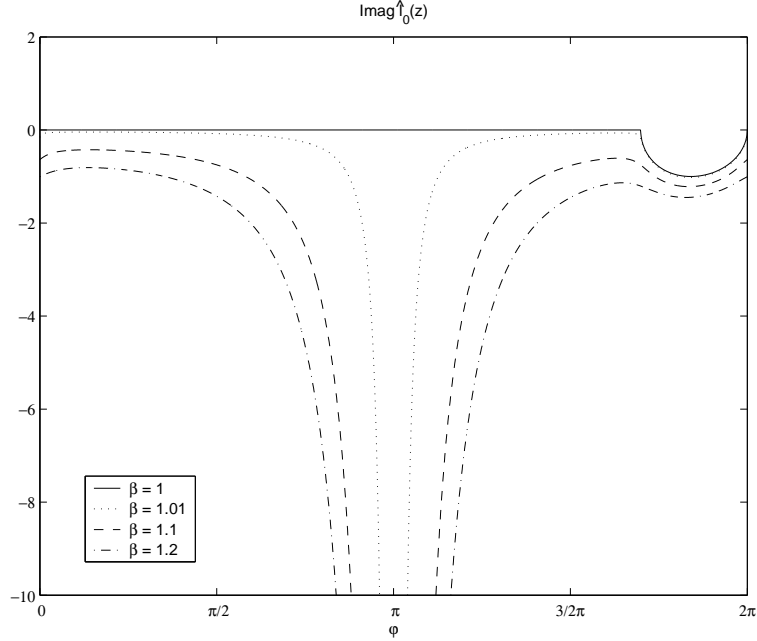


Figure 5: The imaginary part of $\hat{\ell}_0(z)$ is non-positive on the unit circle $z = e^{i\varphi}$, $0 \leq \varphi \leq 2\pi$ (and hence also for $\beta \geq 1$). $\Delta x = 1/160$, $\Delta t = 2 \cdot 10^{-5}$, $V \equiv 0$.

Example 5.4. (Discrete counterpart of Example 5.2) As a second example we consider a simplification of the exact DTBC (1.16), where the convolution coefficients $s_{j,n}$ are cut off for $n \geq N$ (cf. [17] for a discussion of the accuracy and practical relevance of these BCs). The corresponding Z -transform,

$$\hat{\ell}_j^{(N)}(z) = \frac{z}{z+1} \hat{s}_j^{(N)}(z) = \frac{z}{z+1} \sum_{n=0}^N s_{j,n} z^{-n} \quad (5.25)$$

satisfies the growth condition (5.15) only for $\beta \geq 1.25$ if $N = 10$ (see Figure 6). (The continuous analogue of such a cut-off kernel was given in (5.8)).

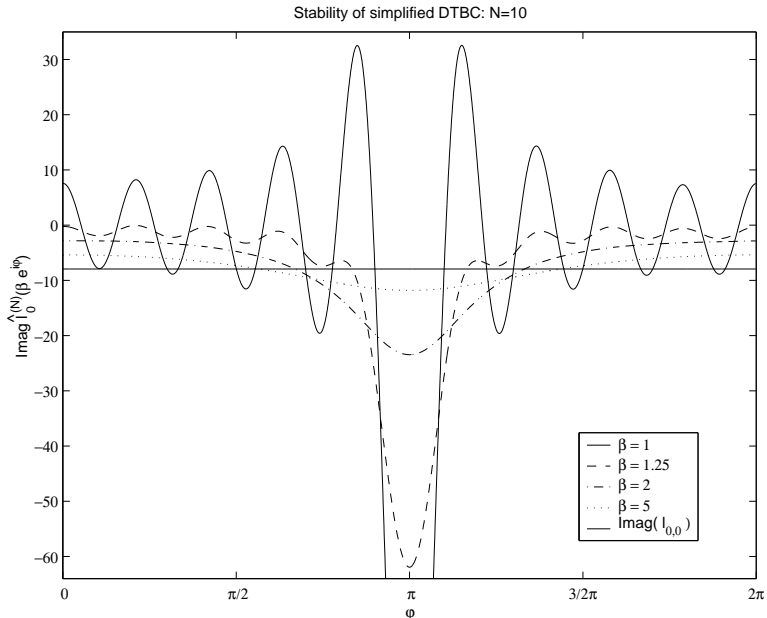


Figure 6: Growth condition $\text{Im } \hat{\ell}_0^{(N)}(z = \beta e^{i\varphi}) \leq 0$ for simplified discrete transparent boundary conditions with cut-off after $N = 10$ convolution coefficients, $\Delta x = 1/160$, $\Delta t = 2 \cdot 10^{-5}$, $V \equiv 0$. The stability condition (5.15) is satisfied for $\beta \geq 1.25$, and $\text{Im } \ell_{0,0} < 0$ holds.

ℓ^2 -stability. Now we turn to the stability of the numerical scheme (5.10) as $\Delta t \rightarrow 0$. To this end we shall derive uniform estimates for $\|\psi_n\|_2$ (as $\Delta t \rightarrow 0$ and $0 \leq n\Delta t \leq T$) by using Lemma 5.1. This lemma bounds the exponential growth of solutions to the numerical scheme for a *fixed* discretization $(\Delta x, \Delta t)$ and it will be applied for each value of Δt along with a corresponding radius $\beta(\Delta t)$. Since the case $\beta(\Delta t) \equiv 1$ is trivial (cf. the DTBC illustrated in Figure 5) we focus on the case when $\beta = \beta(\Delta t) > 1$. For estimating $\|\psi_n\|_2$ we shall require that there exists a fixed $\rho \geq 0$ such that

$$\beta(\Delta t) \leq e^{\rho \Delta t}, \quad \forall 0 < \Delta t \leq \Delta t_0.$$

Using (5.16) this would then yield our final stability estimate

$$\|\psi_n\|_2 \leq \|\psi_0\|_2 \beta(\Delta t)^n \leq \|\psi_0\|_2 e^{\rho n \Delta t} \leq \|\psi_0\|_2 e^{\rho T}, \quad \forall n \Delta t \leq T. \quad (5.26)$$

Next we shall discuss conditions on the boundary function $\hat{g}_j(z)$ for one *fixed* discretization $(\Delta x_0, \Delta t_0)$, which imply that the stability estimate (5.15) holds *for all* $0 < \Delta t \leq \Delta t_0$ on circles with radius $\beta(\Delta t) = e^{\rho \Delta t}$, which decrease as $\Delta t \rightarrow 0$. In the following three cases we shall assume different behaviours of the function $\Delta x = \Delta x(\Delta t)$ (as $\Delta t \rightarrow 0$) that permit to prove stability of the scheme (5.10):

Case 1. $R = 4\Delta x^2/\Delta t = \text{const}$ as $\Delta t \rightarrow 0$, and $V_j = 0$:

Because of the functional dependence (5.12), \hat{g}_j is here independent of Δt , and therefore β in (5.15) would also be independent of Δt . Hence, the stability estimate (5.26) can only be obtained if the condition (5.15) holds for $\beta = \beta(\Delta t_0) = 1$.

Case 2. $\Delta x = \Delta x_0 = \text{const}$ and $V_j \in \mathbb{R}$:

Theorem 5.1. *Let the transformed boundary kernels \hat{g}_0, \hat{g}_J satisfy*

$$\text{Im} \hat{g}_0(z, \Delta x_0, \Delta t_0) \Big|_{\mathcal{C}_1} \leq 0, \quad \text{Im} \hat{g}_J(z, \Delta x_0, \Delta t_0) \Big|_{\mathcal{C}_1} \leq 0 \quad (5.27)$$

for some fixed Δx_0 and Δt_0 . Here, the circle \mathcal{C}_1 is defined by

$$z = \frac{\beta_0 - 1}{2} + \frac{\beta_0 + 1}{2} e^{i\varphi}, \quad 0 \leq \varphi \leq 2\pi,$$

(cf. Figure 7) with some sufficiently large $\beta_0 = e^{\rho \Delta t_0} \geq 1$ (note that $z = -1$ and $z = \beta_0 \in \mathcal{C}_1$).

Then, the stability estimate (5.26) holds for all $0 < \Delta t \leq \Delta t_0$ and $\Delta x = \Delta x_0$.

Proof. Following the above remark (after the proof of Lemma 5.1) we first note that condition (5.27) implies

$$\text{Im} \hat{g}_j(z, \Delta x_0, \Delta t_0) \leq 0 \quad \forall z \in \mathcal{C}_1^o, \quad (5.28)$$

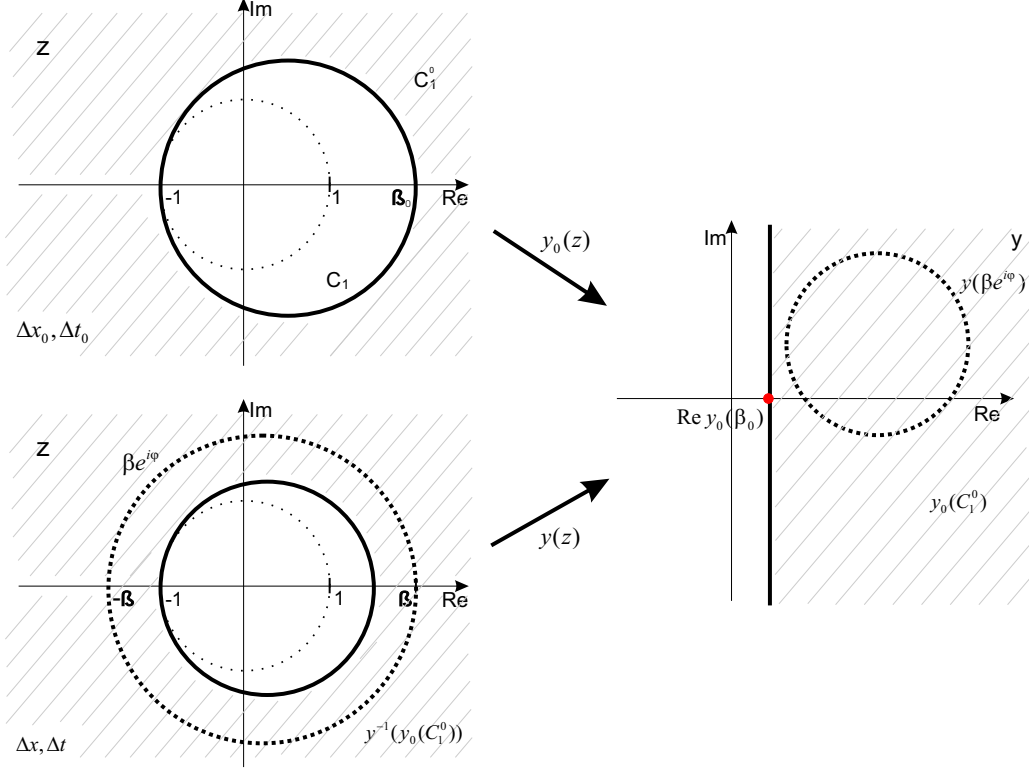


Figure 7: Illustration of the 2 maps $y_0(z)$ and $y(z)$ from the proof of Theorem 5.1: The circle $z = \beta e^{i\varphi}$ (dashed line) is mapped onto $y(\beta e^{i\varphi})$ which lies inside the (shaded) stability region $y_0(C_1^o)$.

where C_1^o denotes the part of the complex plane “outside” of the circle C_1 . The idea of the proof is to conclude that (5.28) implies

$$\text{Im } \hat{g}_j(z = \beta(\Delta t)e^{i\varphi}, \Delta x_0, \Delta t) \leq 0, \quad \forall 0 < \Delta t \leq \Delta t_0, \quad 0 \leq \varphi \leq 2\pi, \quad (5.29)$$

with $\beta(\Delta t) = e^{\rho\Delta t}$. To this end we shall compare the images of C_1^o and the circles $\beta(\Delta t)e^{i\varphi}$ from (5.29) under the respective maps $y_0(z) = y(z, \Delta x_0, \Delta t_0)$ and $y(z) = y(z, \Delta x_0, \Delta t)$ from (5.12).

We first consider the rational map

$$y_0(z) = \frac{2\Delta x_0^2}{\Delta t_0} \left(\frac{z-1}{z+1} + i \frac{\Delta t_0 V_j}{2} \right) : \mathbb{C} \rightarrow \mathbb{C} \quad (5.30)$$

from (5.12). $y_0(\mathcal{C}_1^o)$, the image of \mathcal{C}_1^o is the set $y \in \mathbb{C}$ with

$$\operatorname{Re} y \geq \operatorname{Re} y_0(z = \beta_0) = \frac{2\Delta x_0^2 \beta_0 - 1}{\Delta t_0 \beta_0 + 1} = \frac{2\Delta x_0^2}{\Delta t_0} \tanh \frac{\rho \Delta t_0}{2}. \quad (5.31)$$

In order to verify the estimate (5.15) with $\beta(\Delta t) = e^{\rho \Delta t}$ for $0 < \Delta t \leq \Delta t_0$ we calculate:

$$\hat{g}_j(z = e^{\rho \Delta t + i\varphi}, \Delta x_0, \Delta t) = \hat{h}_j(y(\Delta t, \varphi)), \quad (5.32)$$

with

$$y(\Delta t, \varphi) := \frac{2\Delta x_0^2}{\Delta t} \left[\frac{e^{\rho \Delta t + i\varphi} - 1}{e^{\rho \Delta t + i\varphi} + 1} + i \frac{\Delta t V_j}{2} \right].$$

Using the rational map $y(z) = \frac{2\Delta x_0^2}{\Delta t} \left(\frac{z-1}{z+1} + i \frac{\Delta t V_j}{2} \right)$ we see that

$$\operatorname{Re} y(\Delta t, \varphi) \geq \operatorname{Re} y(\Delta t, 0) = \frac{2\Delta x_0^2}{\Delta t} \tanh \frac{\rho \Delta t}{2}, \quad \forall 0 \leq \varphi \leq 2\pi.$$

Due to the monotonicity of the function $\tanh x/x$ we finally obtain for the argument of \hat{h}_j in (5.32):

$$\operatorname{Re} y(\Delta t, \varphi) \geq \frac{2\Delta x_0^2}{\Delta t_0} \tanh \frac{\rho \Delta t_0}{2} = \operatorname{Re} y_0(z = e^{\rho \Delta t_0} = \beta_0), \quad \forall 0 < \Delta t \leq \Delta t_0, 0 \leq \varphi \leq 2\pi.$$

Hence,

$$y_0^{-1}(y(\Delta t, \varphi)) \in \mathcal{C}_1^o, \quad \forall 0 < \Delta t \leq \Delta t_0, 0 \leq \varphi \leq 2\pi.$$

(5.28) now shows that

$$\operatorname{Im} \hat{g}_j(\beta e^{i\varphi}, \Delta x_0, \Delta t) \leq 0$$

holds with $\beta = e^{\rho \Delta t}$, and (5.26) follows.

Summarizing, the idea of the proof is based on the fact that all circles $\beta(\Delta t)e^{i\varphi}$ (with $0 < \Delta t \leq \Delta t_0$) are mapped via $y_0^{-1} \circ y$ into \mathcal{C}_1^o (cf. Figure 7). \square

Case 3. $\Delta x = \alpha \Delta t^\gamma$ (with $\alpha = \Delta x_0 / \Delta t_0^\gamma$, $\gamma \geq 1$) and $V_j \in \mathbb{R}$:

Theorem 5.2. (a) Let $V_j = 0$ and let the transformed boundary kernels \hat{g}_0, \hat{g}_J satisfy

$$\operatorname{Im} \hat{g}_0(z, \Delta x_0, \Delta t_0) \Big|_{\mathcal{C}_2} \leq 0, \quad \operatorname{Im} \hat{g}_J(z, \Delta x_0, \Delta t_0) \Big|_{\mathcal{C}_2} \leq 0 \quad (5.33)$$

for some Δx_0 and Δt_0 . Here, the circle \mathcal{C}_2 is defined by

$$z = -\frac{\beta_0 - 1}{2} + \frac{\beta_0 + 1}{2} e^{i\varphi}, \quad 0 \leq \varphi \leq 2\pi,$$

and some sufficiently large $\beta_0 = e^{\rho\Delta t_0} \geq 1$ (note that $z = -\beta_0$ and $z = 1 \in \mathcal{C}_2$).

Then, the stability estimate (5.26) holds for all $0 < \Delta t \leq \Delta t_0$ and $\Delta x = \alpha\Delta t^\gamma$.

(b) Let $V_j \in \mathbb{R}$ and let \hat{g}_0^0, \hat{g}_J^0 , the transformed boundary kernels pertaining to $V_j = 0$, satisfy condition (5.33) for some $\Delta x_0, \Delta t_0$, and $\beta_0 = e^{\rho\Delta t_0} \geq 1$.

Then, the stability estimate (5.26) holds for all $0 < \Delta t \leq \Delta t_1$ (with some $0 < \Delta t_1 \leq \Delta t_0$) and $\Delta x = \alpha\Delta t^\gamma$.

Proof. Part (a):

We follow the strategy of the previous proof and first note that condition (5.33) implies

$$\operatorname{Im} \hat{g}_j(z, \Delta x_0, \Delta t_0) \leq 0 \quad \forall z \in \mathcal{C}_2^o, \quad (5.34)$$

where \mathcal{C}_2^o denotes the “outside” of circle \mathcal{C}_2 . $y_0(\mathcal{C}_2^o)$, its image under the rational map

$$y_0(z) = \frac{2\Delta x_0^2}{\Delta t_0} \frac{z - 1}{z + 1} \quad (5.35)$$

is characterized by $y \in \mathbb{C}$ with

$$\left| y + \frac{\Delta x_0^2}{\Delta t_0} \frac{\beta_0 + 1}{\beta_0 - 1} \right| \leq \frac{\Delta x_0^2}{\Delta t_0} \frac{\beta_0 + 1}{\beta_0 - 1}. \quad (5.36)$$

The disk $y_0(\mathcal{C}_2^o)$ is symmetric to the real axis, with left vertex at $y_l = 0$ and right vertex at $y_r = \frac{2\Delta x_0^2}{\Delta t_0} \coth \frac{\rho\Delta t_0}{2}$.

In order to verify the estimate (5.15) with $\beta(\Delta t) = e^{\rho\Delta t}$ for $0 < \Delta t \leq \Delta t_0$ we calculate:

$$\hat{g}_j(z = e^{\rho\Delta t+i\varphi}, \alpha\Delta t^\gamma, \Delta t) = \hat{h}_j(y(\Delta t, \varphi)), \quad (5.37)$$

with

$$y(\Delta t, \varphi) := 2\alpha^2\Delta t^{2\gamma-1} \frac{e^{\rho\Delta t+i\varphi} - 1}{e^{\rho\Delta t+i\varphi} + 1}. \quad (5.38)$$

For fixed $0 < \Delta t \leq \Delta t_0$ the set $\{y(\Delta t, \varphi) \mid 0 \leq \varphi \leq 2\pi\}$ is a circle, lying symmetric to the real axis with left vertex at

$$y(\Delta t, 0) = 2\alpha^2\Delta t^{2\gamma-1} \tanh \frac{\rho\Delta t}{2} > y_l = 0,$$

and right vertex at

$$y(\Delta t, \pi) = 2\alpha^2\Delta t^{2\gamma-1} \coth \frac{\rho\Delta t}{2} \leq y_r.$$

Therefore the circles $\{y(\Delta t, \varphi) \mid 0 \leq \varphi \leq 2\pi\} \subset y_0(\mathcal{C}_2^o)$, for $0 < \Delta t \leq \Delta t_0$.

Hence, (5.34) and (5.36) show that

$$\text{Im } \hat{g}_j(\beta e^{i\varphi}, \Delta x, \Delta t) \leq 0$$

holds with $\beta = e^{\rho\Delta t}$, $\Delta x = \alpha\Delta t^\gamma$, and the stability estimate (5.26) follows.

Part (b):

To verify the estimate (5.15) we have to show that $\text{Im } \hat{g}_j(z = e^{\rho\Delta t+i\varphi}, \alpha\Delta t^\gamma, \Delta t) = \text{Im } \hat{h}_j(y(\Delta t, \varphi)) \leq 0$, with

$$y(\Delta t, \varphi) := 2\alpha^2\Delta t^{2\gamma-1} \left[\frac{e^{\rho\Delta t+i\varphi} - 1}{e^{\rho\Delta t+i\varphi} + 1} + i \frac{\Delta t V_j}{2} \right].$$

The circles $y(\Delta t, \varphi)$, $0 \leq \varphi \leq 2\pi$ are only vertical shifts of the circles (5.38), and their left vertex is at

$$y(\Delta t, 0) = \alpha^2\Delta t^{2\gamma}(\rho + iV_j) + \mathcal{O}(\Delta t^{2\gamma+1}) \quad \text{for } \Delta t \rightarrow 0.$$

Hence, the circles $\{y(\Delta t, \varphi) \mid 0 \leq \varphi \leq 2\pi\} \subset y_0(\mathcal{C}_2^o)$, for $0 < \Delta t \leq \Delta t_1$ (for some $0 < \Delta t_1 \leq \Delta t_0$; cf. Figure 8) and the stability estimate (5.26) follows. □

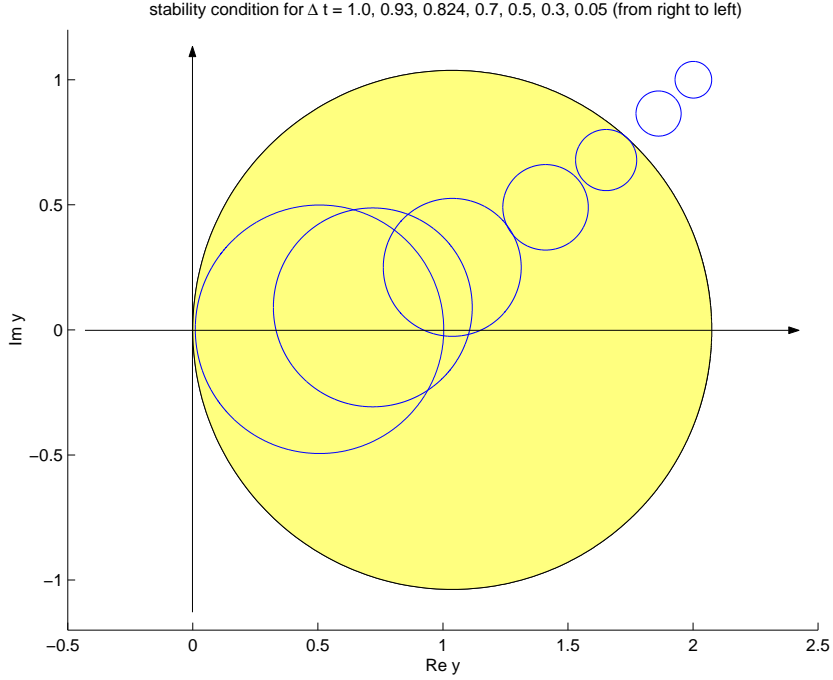


Figure 8: Illustration of the proof of Theorem 5.2 (b): For $\Delta t \leq \Delta t_1 \approx 0.82$ the (small) circles $\{y(\Delta t, \varphi) \mid 0 \leq \varphi \leq 2\pi\}$ are inside the (shaded) stability region $y_0(\mathcal{C}_2^o)$. Parameters: $\Delta x_0 = \Delta t_0 = V = \gamma = 1$, $\rho = 4$.

We now illustrate the stability condition (5.27) of Case 2 and condition (5.33) of Case 3 for the exponential–sum–coefficients introduced in Section 3. The upper left graphic of Figure 7 shows the unit circle (dotted line) in the complex plane and the circle \mathcal{C}_1 (solid line), on which we shall check the stability condition.

Example 5.5. We consider the free 1D–Schrödinger equation with the discretization $\Delta x = 1/160$, $\Delta t = 2 \cdot 10^{-5}$. The transformed boundary kernel has the form $\hat{\ell}(z) = \frac{z}{z+1} \hat{\tilde{s}}(z)$, where the Z–transform of $\{\tilde{s}_n\}$ with $\nu = 2$ reads

$$\hat{\tilde{s}}(z) = s_0 + s_1 z^{-1} + \sum_{l=1}^L \frac{b_l}{q_l z - 1} \frac{1}{q_l z}, \quad |z| \geq 1. \quad (5.39)$$

We recall that $|q_l| > 1$, $l = 1, \dots, L$ (cf. Theorem 3.2(ii)), and hence all poles of $\hat{\tilde{s}}$ are inside the unit circle.

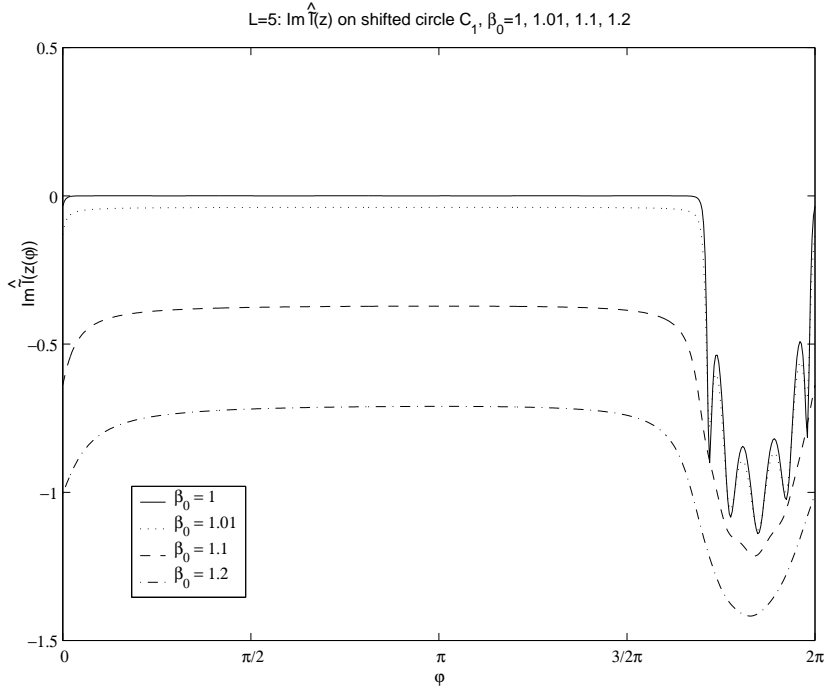


Figure 9: Stability condition $\text{Im } \hat{\ell}|_{C_1} \leq 0$ for exponential-sum-coefficients with $L = 5$. The condition is not satisfied for $\beta_0 = 1$ but is satisfied for $\beta_0 \geq 1.0000008$.

Figure 9 shows $\text{Im } \hat{\ell}|_{C_1}$ for $L = 5$ and various values of β_0 . For $\beta_0 = 1$, $\text{Im } \hat{\ell}$ is not always negative on the unit circle ($\max \text{Im } \hat{\ell}|_{C_1} = 3.064e - 6$ if $L = 5$). Thus the stability condition is not satisfied for $\beta_0 = 1$, but it is satisfied for larger values of β_0 . Comparing these plots with the transformed boundary kernel of the exact DTBC (Figure 5 in Example 5.3) we observe that the ‘valley’ of the graph is at the same position. With increasing β_0 this valley becomes flatter and $\text{Im } \hat{\ell}|_{C_1}$ converges to $\text{Im } s_0 \approx -7.93$.

Note that the imaginary part of $\hat{\ell} = \hat{s} \frac{z}{z+1}$ has no singularity at $z = -1 \in C_1$. This is due to the fact that $\text{Re } \hat{s}(z = -1) = 0$ (cf. (1.11a), (1.11b)) and its (reasonable) approximations (5.39) also satisfy $\text{Re } \hat{s}(z = -1) = 0$. Furthermore, $\text{Re} \frac{z}{z+1}$ is continuous at $z = -1$ on the circle C_1 .

Similarly, Figure 10 shows that condition (5.33), i.e. $\text{Im } \hat{\ell}|_{C_2} \leq 0$ is satis-

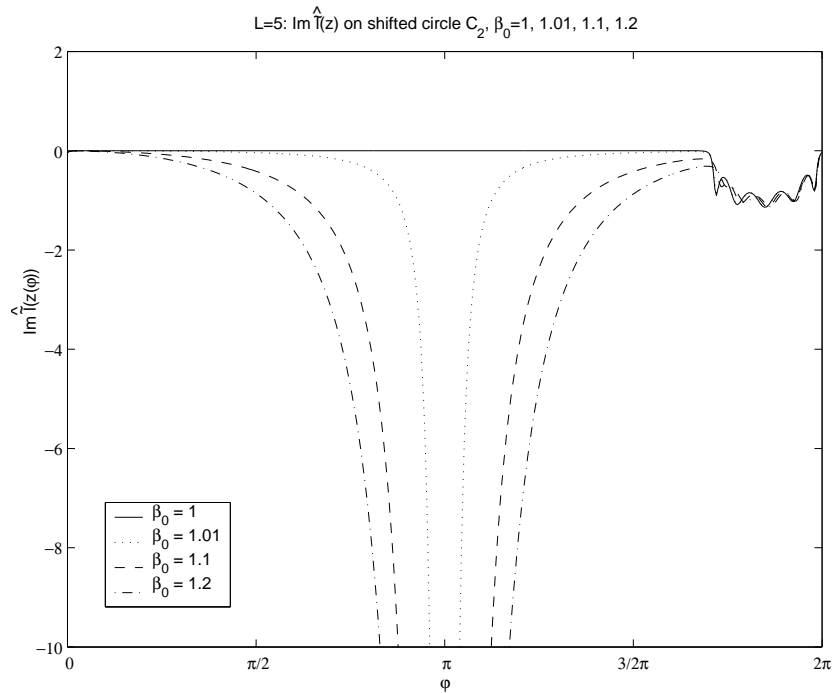


Figure 10: Stability condition $\text{Im } \hat{\ell}|_{C_2} \leq 0$ for exponential-sum-coefficients with $L = 5$. The condition is not satisfied for $\beta_0 = 1$ but is satisfied for $\beta_0 \geq 1.00025$.

fixed for $\beta_0 \geq 1.00025$

Remark. We recognized in this example that $\text{Im } \hat{\ell}$ is positive on parts of the unit circle. This means that some modes of the discretized Schrödinger equation could grow very fast. However, we never observed this in our numerical experiments.

We remark that the stability condition of Theorem 5.1 is independent of the potential V_j in the exterior domain:

Proposition 5.2. *Let the stability condition (5.27) hold on C_1^o for one value of the potential $V_j \in \mathbb{R}$. Then this condition holds on the same circle (i.e. for the same β_0) for all $V_j \in \mathbb{R}$.*

Proof. This result is easily seen from the properties of the map y_0 , defined in

(5.30): Note that y_0 maps \mathcal{C}_1^o onto the half plane $\{y \in \mathbb{C} \mid \operatorname{Re} y > \operatorname{Re} y_0(\beta_0)\}$, independently of V_j (cf. Figure 7). \square

ℓ^2 -stability in 2D. To finish this section we return to the original 2D-problem and discuss the stability properties of the complete scheme (1.4) (for $j = 1, \dots, J-1$) along with the Dirichlet BCs (1.5) and (exact or approximate) DTBCs for each transversal mode ψ^m ; $m = 1, \dots, K-1$:

$$\begin{aligned}\Delta^+ \hat{\psi}_0^m(z) &= (\hat{g}_0^m(z) - 1) \hat{\psi}_0^m(z), \\ \Delta^- \hat{\psi}_J^m(z) &= -(\hat{g}_J^m(z) - 1) \hat{\psi}_J^m(z).\end{aligned}\tag{5.40}$$

Each mode satisfies in the 2 exterior domains a 1D-Schrödinger equation with the effective potential V_j^m ; $j = 0, J$ (cf. (1.6)). If $\hat{g}_j(z)$; $j = 0, J$ are the chosen transformed boundary kernels for the free 1D-Schrödinger equation (i.e. with $V_{\pm} = 0$), the corresponding kernels for the 2D-modes read

$$\hat{g}_j^m(z^*) = \hat{g}_j(z(z^*)) = \hat{g}_j\left(\frac{\tilde{a}z^* + \tilde{b}}{\tilde{a} + \tilde{b}z^*}\right),$$

with $\tilde{a} = 4 - i\Delta t V_j^m$, $\tilde{b} = i\Delta t V_j^m$ (cf. the derivation of the Transformation 3.1).

In fact the stability result of the 1D case readily carries over to 2 dimensions and it is a simple consequence of Proposition 5.2 and of Theorem 5.2(b):

Proposition 5.3. *Let the transformed boundary kernels $\hat{g}_j(z)$; $j = 0, J$ of the free 1D-Schrödinger equation satisfy the conditions of either Theorem 5.1 or Theorem 5.2.*

Then the 2D-Schrödinger scheme (1.4) with the BCs (1.5), (5.40) satisfies the following stability estimate:

$$\begin{aligned}\|\psi_n\|_2 &\leq \|\psi_0\|_2 e^{\rho T}, & \forall n\Delta t \leq T, \\ &\text{with either } 0 < \Delta t \leq \Delta t_0, \Delta x = \Delta x_0, \text{ and } \forall \Delta y > 0, \\ &\text{or } 0 < \Delta t \leq \Delta t_1 (\leq \Delta t_0), \Delta x = \frac{\Delta x_0}{\Delta t_0^\gamma} \Delta t^\gamma (\gamma \geq 1), \text{ and } \Delta y = \Delta y_0 > 0.\end{aligned}$$

6 Error estimates

In this section we consider the numerical scheme for the 1D–Schrödinger equation (1.7) with (approximatively) transparent BCs of convolution form (1.16). We shall derive error estimates for the numerical solution when replacing the exact DTBC by an approximation (like those introduced in §3). First we extend the analytic a-priori estimate of Proposition 5.1 for the continuous IBVP for the Schrödinger equation when modifying the BCs. To this end, let $\psi(x, t)$ solve (5.1) with given functions f_0, f_X satisfying (5.3) for some $\alpha_1 \in \mathbb{R}$.

H¹–a-priori estimate of continuous solution. First we derive an energy estimate for the function $\psi_x(x, t)$:

Proposition 6.1. *Assume that $V_x \in L^2_{loc}(\mathbb{R}_t^+; L^\infty(0, X))$, $\psi^I \in H^1(0, X)$. Let the transformed boundary kernels \hat{f}_0, \hat{f}_X satisfy for some $\alpha_2 \geq 0$:*

$$\operatorname{Re} \left\{ \overline{(s + iV_-)} \hat{f}_0(s) \right\} \geq 0, \quad \operatorname{Re} \left\{ \overline{(s + iV_+)} \hat{f}_X(s) \right\} \leq 0, \quad s = \alpha_2 + i\xi, \quad (6.1)$$

for all $\xi \in \mathbb{R}$. Then the solution ψ of (5.1) satisfies the a-priori estimate

$$\|\psi_x(\cdot, t)\|_{L^2(0, X)}^2 \leq e^{2ct} \left[\|\psi_x^I\|_{L^2(0, X)}^2 + \|\psi^I\|_{L^2(0, X)}^2 V_x^{\max}(t) \right], \quad (6.2)$$

where $V_x^{\max}(t) := \int_0^t e^{2(\alpha_1 - \alpha_2)\tau} \|V_x(\cdot, \tau)\|_{L^\infty(0, X)}^2 d\tau$ and $c = \max(\alpha_2, 1/2)$.

Proof. A simple energy estimate for $\theta(x, t) := \psi_x(x, t)e^{-\alpha_2 t}$, $\alpha_2 \geq 0$, gives

$$\begin{aligned} \frac{d}{dt} \|\theta(\cdot, t)\|_{L^2(0, X)}^2 &= \operatorname{Im} \left\{ \theta(x, t) \bar{\theta}_x(x, t) \right\} \Big|_{x=0}^{x=X} \\ &\quad - 2\alpha_2 \|\theta(\cdot, t)\|_{L^2(0, X)}^2 + 2 \int_0^X V_x(x, t) \operatorname{Im} \left\{ \psi(x, t) e^{-\alpha_2 t} \bar{\theta}(x, t) \right\} dx. \end{aligned} \quad (6.3)$$

Using the Proposition 5.1 we can estimate the last term:

$$\begin{aligned} &2 \int_0^X V_x(x, t) \operatorname{Im} \left\{ \psi(x, t) e^{-\alpha_2 t} \bar{\theta}(x, t) \right\} dx \\ &\leq 2 \|\theta(\cdot, t)\|_{L^2(0, X)} \|\psi(\cdot, t) e^{-\alpha_2 t}\|_{L^2(0, X)} \|V_x(\cdot, t)\|_{L^\infty(0, X)} \\ &\leq \|\theta(\cdot, t)\|_{L^2(0, X)}^2 + \|\psi^I\|_{L^2(0, X)}^2 e^{2(\alpha_1 - \alpha_2)t} \|V_x(\cdot, t)\|_{L^\infty(0, X)}^2. \end{aligned}$$

By integrating in time we obtain from (6.3)

$$\begin{aligned} \|\theta(\cdot, t)\|_{L^2(0, X)}^2 &\leq \|\psi_x^I\|_{L^2(0, X)}^2 + 2(c - \alpha_2) \int_0^t \|\theta(\cdot, \tau)\|_{L^2(0, X)}^2 d\tau \\ &\quad + \|\psi^I\|_{L^2(0, X)}^2 \int_0^t e^{2(\alpha_1 - \alpha_2)\tau} \|V_x(\cdot, \tau)\|_{L^\infty(0, X)}^2 d\tau \\ &\quad + \operatorname{Im} \int_0^t [\bar{\theta}(0, \tau)\theta_x(0, \tau) - \bar{\theta}(X, \tau)\theta_x(X, \tau)] d\tau. \end{aligned} \quad (6.4)$$

It remains to show that the last term in (6.4) is negative. We rewrite the two boundary conditions (5.2)

$$\hat{\psi}_x(0, s) = \hat{f}_0(s)\hat{\psi}(0, s) = \hat{h}_0(s)\hat{\psi}_{xx}(0, s), \quad \hat{h}_0(s) = \frac{\hat{f}_0(s)}{2(V_- - is)}, \quad (6.5a)$$

$$\hat{\psi}_x(X, s) = \hat{f}_X(s)\hat{\psi}(X, s) = \hat{h}_X(s)\hat{\psi}_{xx}(X, s), \quad \hat{h}_X(s) = \frac{\hat{f}_X(s)}{2(V_+ - is)}, \quad (6.5b)$$

$\operatorname{Re} s \geq 0$. Note that ψ_{xx} is not necessarily continuous at $x = 0$, $x = X$. Since the two boundary terms have to be evaluated at $x = 0+$, $x = X-$, the Laplace transformed Schrödinger equation (5.1) was used to replace ψ by $\hat{\psi}_{xx}$ in (6.5).

By again denoting the cut-off function by $\chi_{[0, t]}$ we use Plancherel's identity for Laplace transforms (cf. (5.5)). This gives

$$\begin{aligned} \operatorname{Im} \int_0^t \bar{\theta}(0, \tau)\theta_x(0, \tau) d\tau &= \operatorname{Im} \int_0^\infty \overline{\{(\chi_{[0, t]}\theta_x) * \tilde{h}_0\}(0, \tau)} \chi_{[0, t]}(\tau)\theta_x(0, \tau) d\tau \\ &= -\frac{1}{2\pi} \int_{\mathbb{R}} |\widehat{\chi_{[0, t]}\theta_x}|^2(0, i\xi) \operatorname{Im} \hat{h}_0(\alpha_2 + i\xi) d\xi \leq 0, \end{aligned}$$

provided that (6.1) holds. Here \tilde{h}_0 is given by $\hat{h}_0(s) = \hat{h}_0(\alpha_2 + s)$. An analogous estimate holds for the boundary term at $x = X$. Finally a Gronwall estimate yields the estimate (6.2). \square

Remark. Note that the choice of $\hat{h}_0(s)$, $\hat{h}_X(s)$ in (6.5) is not uncommon; if $\hat{f}_0(s)$, $\hat{f}_X(s)$ correspond to the TBCs (1.2), (1.3) (cf. Example 5.1) then

$$\hat{h}_0(s) = \frac{e^{\frac{\pi}{4}i}}{\sqrt{2}} \frac{1}{\sqrt{s + iV_-}}.$$

An inverse Laplace transformation yields the *impedance boundary condition* [30]:

$$\psi(0, t) = \frac{e^{i\frac{\pi}{4}}}{\sqrt{2\pi}} \int_0^t \frac{\psi_x(0, \tau) e^{-iV_-(t-\tau)}}{\sqrt{t-\tau}} d\tau, \quad (6.6)$$

which is equivalent (for smooth functions) to (1.2).

Combining Propositions 5.1 and 6.1 yields an a-priori estimate for the solution at the boundaries (by using a Sobolev–imbedding):

$$\begin{aligned} & |\psi(0, t)|^2 + |\psi(X, t)|^2 \\ & \leq C \left\{ e^{2\alpha_1 t} \|\psi^I\|_{L^2(0, X)}^2 + e^{2ct} \left[\|\psi_x^I\|_{L^2(0, X)}^2 + \|\psi^I\|_{L^2(0, X)}^2 V_x^{\max}(t) \right] \right\}, \end{aligned} \quad (6.7)$$

where C denotes here and in the sequel generic but not necessarily equal constants.

Example 6.1. (*exact TBC*) We return to the exact TBC of Example 5.1. Its Laplace-transformed kernels \hat{f}_0^{TBC} , \hat{f}_X^{TBC} , satisfy the condition (6.1) for all $\alpha_2 \geq 0$, i.e.

$$\operatorname{Re} \left\{ \overline{(s + iV_-)} \hat{f}_0(s) \right\} = \sqrt{2} \operatorname{Re} \left\{ e^{-\frac{\pi}{4}i} \overline{(s + iV_-)} \sqrt[4]{s + iV_-} \right\} \geq 0, \quad s = \alpha_2 + i\xi, \quad (6.8)$$

holds for all $\xi \in \mathbb{R}$ and analogously for \hat{f}_X^{TBC} . This is easily deduced from $\arg(s + iV_-) \in [-\pi/2, \pi/2]$, which implies $\arg(\overline{(s + iV_-)} \sqrt[4]{s + iV_-}) \in [-\pi/4, \pi/4]$.

Error estimate of continuous solution. Now let $\mu(x, t)$ solve (5.1) with the exact TBC kernels f_0^{TBC} , f_X^{TBC} (cf. Example 5.1) and let $\psi(x, t)$ solve (5.1) with given functions f_0, f_X satisfying (5.3) for some $\alpha_1 \in \mathbb{R}$. Then the error $\kappa(x, t) := \mu(x, t) - \psi(x, t)$ solves the system

$$\begin{cases} i\kappa_t & = -\frac{1}{2}\kappa_{xx} + V(x, t)\kappa, & 0 < x < X, t > 0, \\ \kappa(x, 0) & = 0, & 0 < x < X, \\ \hat{\kappa}_x(0, s) & = \hat{f}_0^{\text{TBC}}(s)\hat{\kappa}(0, s) + [\hat{f}_0^{\text{TBC}}(s) - \hat{f}_0(s)]\hat{\psi}(0, s), & \operatorname{Re} s \geq 0, \\ \hat{\kappa}_x(X, s) & = \hat{f}_X^{\text{TBC}}(s)\hat{\kappa}(X, s) + [\hat{f}_X^{\text{TBC}}(s) - \hat{f}_X(s)]\hat{\psi}(X, s), & \operatorname{Re} s \geq 0, \end{cases} \quad (6.9)$$

and we can formulate the following *error estimate*:

Theorem 6.1. *Let the assumptions of Proposition 6.1 be fulfilled and let $c = \max(\alpha_2, 1/2)$. Then the following estimate holds for all $\alpha \geq 0$, $\alpha \neq \alpha_1$, $\alpha \neq c$:*

$$\begin{aligned} \|\kappa(\cdot, t)\|_{L^2(0, X)}^2 &\leq f_{0, X}^{\max} \left[a_1 (e^{2\alpha_1 t} - e^{2\alpha t}) + a_2 (e^{2ct} - e^{2\alpha t}) \right. \\ &\quad \left. + a_3 (e^{2ct} V_x^{\max}(t) - e^{2\alpha t} \int_0^t e^{2(\alpha_1 - \alpha_2)\tau} \|V_x(\cdot, \tau)\|_{L^\infty(0, X)}^2 e^{2(c-\alpha)\tau} d\tau) \right] \end{aligned} \quad (6.10)$$

with

$$f_{0, X}^{\max} := \|\hat{f}_0^{\text{TBC}}(\alpha + i\xi) - \hat{f}_0(\alpha + i\xi)\|_{L^\infty(\mathbb{R}_\xi)} + \|\hat{f}_X^{\text{TBC}}(\alpha + i\xi) - \hat{f}_X(\alpha + i\xi)\|_{L^\infty(\mathbb{R}_\xi)}$$

and

$$a_1 = \frac{C \|\psi^I\|_{L^2(0, X)}^2}{(\alpha_1 - \alpha)}, \quad a_2 = \frac{C \|\psi_x^I\|_{L^2(0, X)}^2}{(c - \alpha)}, \quad a_3 = \frac{C \|\psi^I\|_{L^2(0, X)}^2}{(c - \alpha)}.$$

For $\alpha = \alpha_1$ or $\alpha = c$ one takes the obvious limits in (6.10).

Proof. As for Proposition 5.1 the theorem is easily proved by using an energy estimate for the function $\eta(x, t) := \kappa(x, t)e^{-\alpha t}$, $\alpha \geq 0$, which satisfies:

$$\begin{cases} i\eta_t &= -\frac{1}{2}\eta_{xx} + (V(x, t) - i\alpha)\eta, & 0 < x < X, t > 0, \\ \eta(x, 0) &= 0, & 0 < x < X, \\ \hat{\eta}_x(0, s) &= \hat{f}_0^{\text{TBC}}(s + \alpha)\hat{\eta}(0, s) + [\hat{f}_0^{\text{TBC}}(s + \alpha) - \hat{f}_0(s + \alpha)]\hat{\psi}(0, s + \alpha), \\ \hat{\eta}_x(X, s) &= \hat{f}_X^{\text{TBC}}(s + \alpha)\hat{\eta}(X, s) + [\hat{f}_X^{\text{TBC}}(s + \alpha) - \hat{f}_X(s + \alpha)]\hat{\psi}(X, s + \alpha), \end{cases} \quad (6.11)$$

with $\text{Re } s \geq 0$. An energy estimate for $\eta(x, t)$ yields:

$$\begin{aligned} \|\eta(\cdot, t)\|_{L^2(0, X)}^2 &= -2\alpha \int_0^t \|\eta(\cdot, \tau)\|_{L^2(0, X)}^2 d\tau \\ &\quad + \text{Im} \int_0^t [\bar{\eta}(0, \tau)\eta_x(0, \tau) - \bar{\eta}(X, \tau)\eta_x(X, \tau)] d\tau. \end{aligned} \quad (6.12)$$

Now Plancherel's identity for Laplace transforms gives

$$\begin{aligned}
& \operatorname{Im} \int_0^t \bar{\eta}(0, \tau) \eta_x(0, \tau) d\tau \\
&= \operatorname{Im} \int_0^\infty \overline{\chi_{[0,t]}(\tau) \eta(0, \tau)} \{(\chi_{[0,t]} \eta) * \hat{f}_0^{\text{TBC}}\}(0, \tau) \\
&\quad + \{(\chi_{[0,t]} \psi e^{-\alpha\tau}) * [\hat{f}_0^{\text{TBC}} - \hat{f}_0]\}(0, \tau) d\tau \\
&= \frac{1}{2\pi} \int_{\mathbb{R}} |\widehat{\chi_{[0,t]} \eta}|^2(0, i\xi) \operatorname{Im} \hat{f}_0^{\text{TBC}}(\alpha + i\xi) \\
&\quad + \operatorname{Im} [\hat{f}_0^{\text{TBC}}(\alpha + i\xi) - \hat{f}_0(\alpha + i\xi)] (\widehat{\chi_{[0,t]} \psi})(0, \alpha + i\xi) (\widehat{\chi_{[0,t]} \eta})(0, i\xi) d\xi
\end{aligned}$$

and analogously for the right boundary term. Here \hat{f}_0 is given by $\hat{f}_0(s) = \hat{f}_0(\alpha + s)$. Since $\operatorname{Im} \hat{f}_0^{\text{TBC}}(\alpha + i\xi) \leq 0$ and $\operatorname{Im} \hat{f}_X^{\text{TBC}}(\alpha + i\xi) \geq 0$ for all $\alpha \geq 0$, $\xi \in \mathbb{R}$ (cf. Example 5.1) we obtain

$$\begin{aligned}
& \|\eta(\cdot, t)\|_{L^2(0, X)}^2 \\
&\leq \|\hat{f}_0^{\text{TBC}}(\alpha + i\xi) - \hat{f}_0(\alpha + i\xi)\|_{L^\infty(\mathbb{R}_\xi)} \|\eta(0, \tau)\|_{L^2(0, t)} \|\psi(0, \tau) e^{-\alpha\tau}\|_{L^2(0, t)} \\
&\quad + \|\hat{f}_X^{\text{TBC}}(\alpha + i\xi) - \hat{f}_X(\alpha + i\xi)\|_{L^\infty(\mathbb{R}_\xi)} \|\eta(X, \tau)\|_{L^2(0, t)} \|\psi(X, \tau) e^{-\alpha\tau}\|_{L^2(0, t)}.
\end{aligned}$$

It only remains to estimate the above boundary terms. Using the estimate (6.7) we obtain

$$\begin{aligned}
|\eta(0, t)|^2 &= e^{-2\alpha t} |\mu(0, t) - \psi(0, t)|^2 \\
&\leq C e^{-2\alpha t} \left\{ e^{2\alpha_1 t} \|\psi^I\|_{L^2(0, X)}^2 + e^{2ct} \left[\|\psi_x^I\|_{L^2(0, X)}^2 + \|\psi^I\|_{L^2(0, X)}^2 V_x^{\max}(t) \right] \right\}
\end{aligned}$$

and analogously for $|\eta(X, t)|^2$. Integrating in time yields

$$\begin{aligned}
\|\eta(0, \cdot)\|_{L^2(0, t)}^2 &\leq a_1 (e^{2(\alpha_1 - \alpha)t} - 1) + a_2 (e^{2(c - \alpha)t} - 1) \\
&\quad + a_3 (e^{2(c - \alpha)t} V_x^{\max}(t) - \int_0^t e^{2(\alpha_1 - \alpha_2)\tau} \|V_x(\cdot, \tau)\|_{L^\infty(0, X)}^2 e^{2(c - \alpha)\tau} d\tau) \quad (6.13)
\end{aligned}$$

and an estimate of the same form holds for $\|\psi(X, \tau) e^{-\alpha\tau}\|_{L^2(0, t)}$, i.e. we obtain the estimate (6.10). \square

To illustrate this result we now consider two simple examples:

Example 6.2. (“cut-off” TBC) We continue the discussion of Example 5.2 with the approximate BC-kernel

$$f_0(t) = f_0^{\text{TBC}}(t) H(T - t).$$

Analogously to the procedure in Example 5.2 one can verify numerically that its Laplace transform

$$\hat{f}_0(s) = \sqrt{2} e^{-\frac{\pi}{4}i} \sqrt[4]{s + iV_-} + \frac{1}{\sqrt{2\pi}} e^{-\frac{\pi}{4}i} \int_T^\infty t^{-\frac{3}{2}} e^{-st} dt, \quad s = \alpha_2 + i\xi, \quad \xi \in \mathbb{R},$$

satisfies the condition (6.1) (with $V_- = 0$) for $\tilde{\alpha}_2 \geq 0.25$ if $T = 1$.

Next we verify that the two kernels f_0^{TBC} and f_0 satisfy an error estimate like those appearing on the right hand side of (6.10). These two kernels satisfy

$$\|f_0^{\text{TBC}} - f_0\|_{L^1(0,\infty)} = \sqrt{\frac{2}{\pi T}},$$

and hence

$$\|\hat{f}_0^{\text{TBC}}(\alpha + i\xi) - \hat{f}_0(\alpha + i\xi)\|_{L^\infty(\mathbb{R}_\xi)} \leq \sqrt{\frac{2}{\pi T}} e^{-\alpha T}$$

holds for all $\alpha \geq 0$.

Example 6.3. (rational function kernel) As a second example assume now that \hat{f}_0 is a rational function (as proposed in [3, 10, 14]):

$$\hat{f}_0(s) = \frac{P_{L-1}(s)}{Q_L(s)}.$$

Since $\hat{f}_0^{\text{TBC}}(s) = \sqrt{2} e^{-\frac{\pi}{4}i} \sqrt[4]{s}$ and $\hat{f}_0(s)$ have different asymptotic behaviours for large $|s|$, we conclude

$$\hat{f}_0^{\text{TBC}}(\alpha + i\xi) - \hat{f}_0(\alpha + i\xi) \notin L^\infty(\mathbb{R}_\xi)$$

for any $\alpha \geq 0$. Hence Theorem 6.1 does not apply. We remark that this difficulty will not arise for the discrete BCs with exponential-sum-coefficients derived in §3 (cf. Example 6.5).

h^1 -a-priori estimate of discrete solution. Analogously to the continuous case let $\psi_{j,n}$ solve the Crank–Nicolson scheme (5.10) with \hat{g}_0, \hat{g}_J satisfying (5.15) for some $\beta = \beta_1 \geq 1$. From now on we shall assume that $V_j = V_-$ for $j \leq 1$ and $V_j = V_+$ for $j \geq J - 1$ in addition to the assumptions in §5. First we derive a *discrete h^1 -estimate* of the solution of (5.10) which is the discrete analogue of Proposition 6.1:

Proposition 6.2. *Let the transformed boundary transfer functions \hat{g}_0, \hat{g}_J satisfy the following condition for some (sufficiently large) $\beta_2 \geq 1$:*

$$\operatorname{Re} \left\{ \bar{y}_1(\beta_2 e^{i\varphi}) \left[1 - \frac{1}{\hat{g}_0(\beta_2 e^{i\varphi})} \right] \right\} \geq 0, \quad 0 \leq \varphi \leq 2\pi, \quad (6.14a)$$

$$\operatorname{Re} \left\{ \bar{y}_{J-1}(\beta_2 e^{i\varphi}) \left[1 - \frac{1}{\hat{g}_J(\beta_2 e^{i\varphi})} \right] \right\} \geq 0, \quad 0 \leq \varphi \leq 2\pi, \quad (6.14b)$$

with

$$y_j(z) = \frac{R}{2} \left(\frac{z-1}{z+1} + i\nu_j \right), \quad \nu_1 = \frac{\Delta t V_-}{2}, \quad \nu_{J-1} = \frac{\Delta t V_+}{2}. \quad (6.15)$$

Assume also that \hat{g}_0, \hat{g}_J are analytic for $|z| \geq \beta_2$. Then the following estimate holds for $\Delta t < 2$, $n \in \mathbb{N}$:

$$\|\Delta^+ \psi_n\|_{2,*}^2 \leq c^{2n} \left[\|\Delta^+ \psi_0\|_{2,*}^2 + \frac{(1+\beta_1)^2}{2\beta_2^2} \frac{\|\psi_0\|_2^2}{2-\Delta t} V_{\Delta^+,n-1}^{\max} \right], \quad (6.16)$$

where

$$V_{\Delta^+,n}^{\max} := \Delta t \sum_{k=0}^n \left(\frac{\beta_1}{\beta_2} \right)^{2k} \|\Delta^+ V_{k+\frac{1}{2}}\|_{\infty}^2, \quad c = \max \left(\beta_2, \sqrt{\frac{2+\Delta t}{2-\Delta t}} \right)$$

and the discrete norms are defined by

$$\|\Delta^+ \psi_n\|_{2,*}^2 = \Delta x \sum_{j=1}^{J-2} |\Delta^+ \psi_{j,n}|^2, \quad \|\Delta^+ V_{n+\frac{1}{2}}\|_{\infty} = \max_{j=1,\dots,J-2} |\Delta^+ V_{j,n+\frac{1}{2}}|.$$

(Note the difference to the discrete L^2 -norm in (5.14).)

Proof. The proof is based on a discrete energy estimate for the new variable

$$\theta_{j,n} := \beta_2^{-n} \Delta^+ \psi_{j,n},$$

which solves the equation

$$\begin{aligned} -iR(\theta_{j,n+1} - \theta_{j,n}) &= (\Delta^2 - wV_{j,n+\frac{1}{2}})(\theta_{j,n+1} + \theta_{j,n}) \\ &+ (\beta_2^{-1} - 1)(\Delta^2 - wV_{j,n+\frac{1}{2}} - iR)\theta_{j,n} \\ &- w\beta_2^{-n-1}(\psi_{j+1,n+1} + \psi_{j+1,n}) \Delta^+ V_{j,n+\frac{1}{2}}. \end{aligned} \quad (6.17a)$$

Alternatively this can be written as

$$\begin{aligned} -iR(\theta_{j,n+1} - \theta_{j,n}) &= (\Delta^2 - wV_{j,n+\frac{1}{2}})(\theta_{j,n+1} + \theta_{j,n}) \\ &+ (\beta_2 - 1)(\Delta^2 - wV_{j,n+\frac{1}{2}} + iR)\theta_{j,n+1} \\ &- w\beta_2^{-n}(\psi_{j+1,n+1} + \psi_{j+1,n}) \Delta^+ V_{j,n+\frac{1}{2}}, \end{aligned} \quad (6.17b)$$

for $j = 1, \dots, J-2$ together with the initial condition

$$\theta_{j,0} = \Delta^+ \psi_{j,0}, \quad j = 1, \dots, J-2,$$

and the two transformed boundary conditions

$$\hat{\theta}_0(z) = [\hat{g}_0(\beta_2 z) - 1] \hat{\psi}_0(\beta_2 z), \quad (6.18a)$$

$$\hat{\theta}_{J-1}(z) = -[\hat{g}_J(\beta_2 z) - 1] \hat{\psi}_J(\beta_2 z). \quad (6.18b)$$

We multiply equation (6.17a) with $\bar{\theta}_{j,n}$ and the complex conjugate of (6.17b) with $-\theta_{j,n+1}$ and sum it up for $j = 1, \dots, J-2$. After a lengthy calculation one obtains the following formula:

$$\begin{aligned} \|\theta_{n+1}\|_{2,*}^2 - \|\theta_n\|_{2,*}^2 &= \frac{\Delta t}{4\beta_2^2 \Delta x} \operatorname{Im} [(\bar{\theta}_{0,n} + \beta_2 \bar{\theta}_{0,n+1}) \Delta^+ (\theta_{0,n} + \beta_2 \theta_{0,n+1}) \\ &\quad - (\bar{\theta}_{J-1,n} + \beta_2 \bar{\theta}_{J-1,n+1}) \Delta^- (\theta_{J-1,n} + \beta_2 \theta_{J-1,n+1})] \\ &- (1 - \beta_2^{-2}) \|\theta_n\|_{2,*}^2 \\ &+ \frac{\Delta t \Delta x}{2\beta_2^{n+2}} \sum_{j=1}^{J-2} \operatorname{Im} [(\bar{\theta}_{j,n} + \beta_2 \bar{\theta}_{j,n+1}) (\psi_{j+1,n+1} + \psi_{j+1,n})] \Delta^+ V_{j,n+\frac{1}{2}}, \end{aligned}$$

which is the discrete analogue of (6.3). We estimate the last term using Lemma 5.1

$$\begin{aligned}
& \Delta x \sum_{j=1}^{J-2} \operatorname{Im} [(\bar{\theta}_{j,n} + \beta_2 \bar{\theta}_{j,n+1}) \beta_2^{-n} (\psi_{j+1,n+1} + \psi_{j+1,n})] \Delta^+ V_{j,n+\frac{1}{2}} \\
& \leq \|\theta_n + \beta_2 \theta_{n+1}\|_{2,*} \beta_2^{-n} \|\psi_{n+1} + \psi_n\|_2 \|\Delta^+ V_{n+\frac{1}{2}}\|_\infty \\
& \leq \|\theta_n + \beta_2 \theta_{n+1}\|_{2,*} (1 + \beta_1) \|\psi_0\|_2 \left(\frac{\beta_1}{\beta_2}\right)^n \|\Delta^+ V_{n+\frac{1}{2}}\|_\infty \\
& \leq \|\theta_n\|_{2,*}^2 + \beta_2^2 \|\theta_{n+1}\|_{2,*}^2 + \frac{(1 + \beta_1)^2}{2} \|\psi_0\|_2^2 \left(\frac{\beta_1}{\beta_2}\right)^{2n} \|\Delta^+ V_{n+\frac{1}{2}}\|_\infty^2
\end{aligned}$$

and we obtain

$$\begin{aligned}
\|\theta_{n+1}\|_{2,*}^2 - \|\theta_n\|_{2,*}^2 & \leq \left(\beta_2^{-2} - 1 + \frac{\Delta t}{2\beta_2^2}\right) \|\theta_n\|_{2,*}^2 + \frac{\Delta t}{2} \|\theta_{n+1}\|_{2,*}^2 \\
& \quad + \frac{\Delta t}{4\beta_2^2} (1 + \beta_1)^2 \|\psi_0\|_2^2 \left(\frac{\beta_1}{\beta_2}\right)^{2n} \|\Delta^+ V_{n+\frac{1}{2}}\|_\infty^2 \\
& \quad + \frac{\Delta t}{4\beta_2^2 \Delta x} \operatorname{Im} [(\bar{\theta}_{0,n} + \beta_2 \bar{\theta}_{0,n+1}) \Delta^+ (\theta_{0,n} + \beta_2 \theta_{0,n+1}) \\
& \quad \quad - (\bar{\theta}_{J-1,n} + \beta_2 \bar{\theta}_{J-1,n+1}) \Delta^- (\theta_{J-1,n} + \beta_2 \theta_{J-1,n+1})].
\end{aligned}$$

Summing for $n = 0, \dots, N$ yields

$$\begin{aligned}
\left(1 - \frac{\Delta t}{2}\right) \|\theta_{N+1}\|_{2,*}^2 & \leq -\left(1 - \frac{\Delta t}{2}\right) \sum_{n=1}^N \|\theta_n\|_{2,*}^2 + \left(1 + \frac{\Delta t}{2}\right) \beta_2^{-2} \sum_{n=0}^N \|\theta_n\|_{2,*}^2 \\
& \quad + \frac{(1 + \beta_1)^2}{4\beta_2^2} \|\psi_0\|_2^2 V_{\Delta^+, N}^{\max} \\
& \quad + \frac{\Delta t}{4\beta_2^2 \Delta x} \operatorname{Im} \sum_{n=0}^N [(\bar{\theta}_{0,n} + \beta_2 \bar{\theta}_{0,n+1}) \Delta^+ (\theta_{0,n} + \beta_2 \theta_{0,n+1}) \\
& \quad \quad - (\bar{\theta}_{J-1,n} + \beta_2 \bar{\theta}_{J-1,n+1}) \Delta^- (\theta_{J-1,n} + \beta_2 \theta_{J-1,n+1})].
\end{aligned} \tag{6.19}$$

It remains to determine the sign of the last term in (6.19). To this end,

we rewrite the two boundary conditions (6.18):

$$\hat{\theta}_0(z) = \left[1 - \frac{1}{\hat{g}_0(\beta_2 z)}\right] \hat{\psi}_1(\beta_2 z) = \hat{h}_0(z) \Delta^+ \hat{\theta}_0(z), \quad (6.20a)$$

$$\hat{\theta}_{J-1}(z) = -\left[1 - \frac{1}{\hat{g}_J(\beta_2 z)}\right] \hat{\psi}_{J-1}(\beta_2 z) = \hat{h}_J(z) \Delta^- \hat{\theta}_{J-1}(z), \quad (6.20b)$$

with

$$\hat{h}_0(z) = \frac{1 - \frac{1}{\hat{g}_0(\beta_2 z)}}{-iR \frac{\beta_2 z - 1}{\beta_2 z + 1} + wV_-}, \quad \hat{h}_J(z) = \frac{-\left[1 - \frac{1}{\hat{g}_J(\beta_2 z)}\right]}{-iR \frac{\beta_2 z - 1}{\beta_2 z + 1} + wV_+}. \quad (6.21)$$

As in Section 5 we define (for N fixed) the two sequences,

$$u_n := \begin{cases} \Delta^+(\theta_{0,n} + \beta_2 \theta_{0,n+1}), & n = 0, \dots, N, \\ 0, & n > N, \end{cases}$$

$$v_n := u_n * \tilde{h}_{0,n}, \quad n \in \mathbb{N}_0, \quad \tilde{h}_{0,n} = \mathcal{Z}^{-1}\{\hat{h}_0(z)\}.$$

Now using Plancherel's Theorem for Z -transforms we can show that

$$\begin{aligned} & \operatorname{Im} \sum_{n=0}^N \left[(\bar{\theta}_{0,n} + \beta_2 \bar{\theta}_{0,n+1}) \Delta^+(\theta_{0,n} + \beta_2 \theta_{0,n+1}) \right] \\ &= \operatorname{Im} \sum_{n=0}^N \bar{v}_n u_n = -\operatorname{Im} \sum_{n=0}^{\infty} v_n \bar{u}_n = -\frac{1}{2\pi} \int_0^{2\pi} |\hat{u}(e^{i\varphi})|^2 \operatorname{Im} \hat{h}_0(e^{i\varphi}) d\varphi \end{aligned}$$

is negative since

$$\operatorname{Im} \hat{h}_0(e^{i\varphi}) = \operatorname{Im} \frac{i}{2} \frac{1 - \frac{1}{\hat{g}_0(\beta_2 e^{i\varphi})}}{y_1(\beta_2 e^{i\varphi})} = \frac{\operatorname{Re} \left\{ \bar{y}_1(\beta_2 e^{i\varphi}) \left[1 - \frac{1}{\hat{g}_0(\beta_2 e^{i\varphi})}\right] \right\}}{2|y_1(\beta_2 e^{i\varphi})|^2} \geq 0$$

due to the assumption (6.14). An analogous estimate holds for the right boundary term.

Finally (6.19) yields for $\Delta t < 2$

$$\|\theta_{N+1}\|_{2,*}^2 \leq \|\theta_0\|_{2,*}^2 + \frac{(1 + \beta_1)^2}{2\beta_2^2} \frac{\|\psi_0\|_2^2}{2 - \Delta t} V_{\Delta^+, N}^{\max} + \left(\frac{2 + \Delta t}{2 - \Delta t} \beta_2^{-2} - 1 \right) \sum_{n=0}^N \|\theta_n\|_{2,*}^2. \quad (6.22)$$

With the *discrete Gronwall-type estimate* [31, Lemma 1.4.2] for the function $\|\theta_{N+1}\|_{2,*}^2$ we obtain:

$$\|\theta_{N+1}\|_{2,*}^2 \leq \left(\frac{2 + \Delta t}{2 - \Delta t} \beta_2^{-2}\right)^{N+1} \left[\|\theta_0\|_{2,*}^2 + \frac{(1 + \beta_1)^2}{2\beta_2^2} \frac{\|\psi_0\|_2^2}{2 - \Delta t} V_{\Delta^+, N}^{\max} \right] \quad (6.23)$$

provided that $(2 + \Delta t)/(2 - \Delta t) \geq \beta_2^2$. This yields the estimate (6.16). \square

By combining Lemma 5.1 and Proposition 6.2 and using the discrete Sobolev–inequality

$$|\psi_{j,n}|^2 \leq C(X) \left\{ \|\psi_n\|_2^2 + (\Delta x)^{-2} \|\Delta^+ \psi_n\|_{2,*}^2 \right\}, \quad j = 1, \dots, J-1, \quad (6.24)$$

we now obtain an a-priori pointwise estimate for the discrete solution:

$$|\psi_{j,n}|^2 \leq C(X) \left\{ \beta_1^{2n} \|\psi_0\|_2^2 + c^{2n} (\Delta x)^{-2} \left[\|\Delta^+ \psi_0\|_2^2 + \frac{(1 + \beta_1)^2}{2\beta_2^2} \frac{\|\psi_0\|_2^2}{2 - \Delta t} V_{\Delta^+, n-1}^{\max} \right] \right\} \quad (6.25)$$

for $j = 1, \dots, J-1$, $n \in \mathbb{N}$. Note that this is a discrete analogue of (6.7).

Example 6.4. (*exact DTBC*) We consider the exact DTBC of Example 5.3. The Z -transformed boundary kernel

$$\hat{g}_0^{\text{TBC}}(z) = \hat{\ell}_0(z) = 1 - iy_1(z) + \sqrt{-y_1(z)(y_1(z) + 2i)}$$

(with the branch of the square root chosen such that $|\hat{\ell}_0(z)| \geq 1$) satisfies the condition (6.14) for all $\beta_2 \geq 1$. To verify this, one has to check that

$$\operatorname{Re} \left\{ \bar{y}_1 \left[iy_1 + \sqrt{-y_1(y_1 + 2i)} \right] \right\} = \operatorname{Re} \left\{ \bar{y}_1 \sqrt{-y_1(z)(y_1 + 2i)} \right\} \geq 0 \quad (6.26)$$

holds for all $y_1 = y_1(z)$ with $\operatorname{Re} y_1 \geq 0$ (cf. Figure 7): For $\beta_2 = 1$ (i.e. $\operatorname{Re} y_1 = 0$) this is easily done analytically, and for $\beta_2 > 1$ one can do it numerically. Note that (6.26) is the analogue of (6.8) for the exact DTBC.

Error estimate of discrete solution. Now let $\mu_{j,n}$ be the solution of (5.10) with the exact TBC kernels $\hat{g}_0^{\text{TBC}} = \hat{\ell}_0$, $\hat{g}_J^{\text{TBC}} = \hat{\ell}_J$ (cf. (1.9)) and let $\psi_{j,n}$ solve the Crank–Nicolson scheme (5.10) with other transformed kernels \hat{g}_0 , \hat{g}_J

$$\begin{aligned}
-iR(\eta_{j,n+1} - \eta_{j,n}) &= \Delta^2(\eta_{j,n+1} + \eta_{j,n}) - wV_{j,n+\frac{1}{2}}(\eta_{j,n+1} + \eta_{j,n}) \\
&\quad + (\beta - 1)(\Delta^2 - wV_{j,n+\frac{1}{2}} + iR)\eta_{j,n+1},
\end{aligned} \tag{6.29b}$$

for $j = 1, \dots, J-1$ and the two boundary conditions

$$\Delta^+ \hat{\eta}_0(z) = [\hat{g}_0^{\text{TBC}}(\beta z) - 1] \hat{\eta}_0(z) + [\hat{g}_0^{\text{TBC}}(\beta z) - \hat{g}_0(\beta z)] \hat{\psi}_0(\beta z), \tag{6.30a}$$

$$\Delta^- \hat{\eta}_J(z) = -[\hat{g}_J^{\text{TBC}}(\beta z) - 1] \hat{\eta}_J(z) - [\hat{g}_J^{\text{TBC}}(\beta z) - \hat{g}_J(\beta z)] \hat{\psi}_J(\beta z). \tag{6.30b}$$

We multiply equation (6.29a) with $\bar{\eta}_{j,n}$, the complex conjugate of (6.29b) with $\eta_{j,n+1}$ and sum it up for $j = 1, \dots, J-1$. This gives finally

$$\begin{aligned}
-iR \sum_{j=1}^{J-1} |\eta_{j,n+1}|^2 - |\eta_{j,n}|^2 &= \sum_{j=1}^{J-1} \bar{\eta}_{j,n} \Delta^2(\eta_{j,n+1} + \eta_{j,n}) - \sum_{j=1}^{J-1} \eta_{j,n+1} \Delta^2(\bar{\eta}_{j,n+1} + \bar{\eta}_{j,n}) \\
&\quad + (\beta^{-1} - 1) \sum_{j=1}^{J-1} \bar{\eta}_{j,n} \Delta^2 \eta_{j,n} - (\beta - 1) \sum_{j=1}^{J-1} \eta_{j,n+1} \Delta^2 \bar{\eta}_{j,n+1} \\
&\quad - (\beta^{-1} - 1) iR \sum_{j=1}^{J-1} |\eta_{j,n}|^2 + (\beta - 1) iR \sum_{j=1}^{J-1} |\eta_{j,n+1}|^2 \\
&\quad + w \sum_{j=1}^{J-1} V_{j,n+\frac{1}{2}} (\beta |\eta_{j,n+1}|^2 - \beta^{-1} |\eta_{j,n}|^2).
\end{aligned}$$

After a lengthy calculation one obtains the following expression for the discrete L^2 -norm of the error:

$$\begin{aligned}
\|\eta_{N+1}\|_2^2 &= \frac{1 - \beta^2}{\beta^2} \sum_{n=1}^N \|\eta_n\|_2^2 \\
&\quad + \frac{\Delta t}{4\beta^2 \Delta x} \text{Im} \sum_{n=0}^N \left[(\bar{\eta}_{0,n} + \beta \bar{\eta}_{0,n+1}) \Delta^+ (\eta_{0,n} + \beta \eta_{0,n+1}) \right. \\
&\quad \quad \left. - (\bar{\eta}_{J,n} + \beta \bar{\eta}_{J,n+1}) \Delta^- (\eta_{J,n} + \beta \eta_{J,n+1}) \right].
\end{aligned} \tag{6.31}$$

Since $\beta \geq 1$ it only remains to estimate the boundary terms in (6.31). To this end, we rewrite the two boundary conditions (6.30):

$$\Delta^- \hat{\eta}_1(z) = \hat{h}_0(z) \hat{\eta}_1(z) + \hat{k}_0(z) \hat{\psi}_1(\beta z), \tag{6.32a}$$

$$\Delta^+ \hat{\eta}_{J-1}(z) = -\hat{h}_J(z) \hat{\eta}_{J-1}(z) - \hat{k}_J(z) \hat{\psi}_{J-1}(\beta z). \tag{6.32b}$$

with

$$\hat{h}_j(z) = 1 - \frac{1}{\hat{g}_j^{\text{TBC}}(\beta z)}, \quad \hat{k}_j(z) = \frac{1}{\hat{g}_j(\beta z)} - \frac{1}{\hat{g}_j^{\text{TBC}}(\beta z)}, \quad j = 0, J. \quad (6.33)$$

Again we define (for N fixed) the three sequences,

$$u_n := \begin{cases} \eta_{1,n} + \beta \eta_{1,n+1}, & n = 0, \dots, N, \\ 0, & n > N, \end{cases} \quad w_n := \begin{cases} \psi_{1,n} + \beta \psi_{1,n+1}, & n = 0, \dots, N, \\ 0, & n > N, \end{cases}$$

and

$$v_n := u_n * \tilde{h}_{0,n} + \tilde{k}_{0,n} * w_n, \quad n \in \mathbb{N}_0,$$

where

$$\tilde{h}_{0,n} = \mathcal{Z}^{-1}\{\hat{h}_0(z)\}, \quad \tilde{k}_{0,n} = \mathcal{Z}^{-1}\{\hat{k}_0(z)\}.$$

Using Plancherel's Theorem for Z -transforms we can now show that

$$\begin{aligned} & \Delta t \operatorname{Im} \sum_{n=0}^N (\bar{\eta}_{0,n} + \beta \bar{\eta}_{0,n+1}) \Delta^+ (\eta_{0,n} + \beta \eta_{0,n+1}) \\ &= \Delta t \operatorname{Im} \sum_{n=0}^N (\bar{\eta}_{1,n} + \beta \bar{\eta}_{1,n+1}) \Delta^- (\eta_{1,n} + \beta \eta_{1,n+1}) = \Delta t \operatorname{Im} \sum_{n=0}^{\infty} \bar{u}_n v_n \quad (6.34) \\ &= \frac{\Delta t}{2\pi} \int_0^{2\pi} |\hat{u}(e^{i\varphi})|^2 \operatorname{Im} \hat{h}_0(e^{i\varphi}) + \operatorname{Im} \left\{ \hat{k}_0(e^{i\varphi}) \hat{w}(\beta e^{i\varphi}) \bar{\hat{u}}(e^{i\varphi}) \right\} d\varphi \\ &\leq (1 + \beta)^2 \left\| \hat{k}_0(e^{i\varphi}) \right\|_{L^\infty(0, 2\pi)} \left\| \beta^{-n} \psi_1 \right\|_{\ell^2(0, N)} \|\eta_1\|_{\ell^2(0, N)}, \end{aligned}$$

since $\operatorname{Im} \hat{h}_0(e^{i\varphi}) \leq 0$ for all $\beta \geq 1$. An analogous estimate holds for the right boundary term. The discrete L^2 -norm in (6.34) is defined by $\|\eta_j\|_{\ell^2(0, N)} = \Delta t \sum_{n=0}^N |\eta_{j,n}|^2$. For estimating the boundary term $\|\eta_1\|_{\ell^2(0, N)}$ we use (6.25):

$$\begin{aligned} |\eta_{1,n}|^2 &= \beta^{-2n} |\mu_{1,n} - \psi_{1,n}|^2 \\ &\leq 2 \left\{ \left(\frac{\beta_1}{\beta} \right)^{2n} \|\psi_0\|_2^2 + \left(\frac{c}{\beta} \right)^{2n} X \left[\|\Delta^+ \psi_0\|_2^2 + \frac{(1 + \beta_1)^2}{2\beta_2^2} \frac{\|\psi_0\|_2^2}{2 - \Delta t} V_{\Delta^+, n-1}^{\max} \right] \right\} \quad (6.35) \end{aligned}$$

$n = 0, \dots, N + 1$. Summing for $n = 0, \dots, N$ yields

$$\begin{aligned} \|\eta_1\|_{\ell^2(0,N)}^2 &\leq 2\Delta t \left\{ \frac{1 - \left(\frac{\beta_1}{\beta}\right)^{2(N+1)}}{1 - \frac{\beta_1^2}{\beta^2}} \|\psi_0\|_2^2 + \frac{1 - \left(\frac{c}{\beta}\right)^{2(N+1)}}{1 - \frac{c^2}{\beta^2}} X \|\Delta^+ \psi_0\|_2^2 \right. \\ &\quad \left. + X \frac{(1 + \beta_1)^2}{2\beta_2^2} \frac{\|\psi_0\|_2^2}{2 - \Delta t} \sum_{n=0}^N \left(\frac{c}{\beta}\right)^{2n} V_{\Delta^+, n-1}^{\max} \right\} \end{aligned} \quad (6.36)$$

and an analogous estimate holds for $\|\beta^{-n}\psi_1\|_{\ell^2(0,N)}$, i.e. we obtain (6.28). \square

Remark. Instead of the discrete Sobolev–inequality (6.25) one could also use the following trivial L^2 –estimates in (6.36):

$$|\eta_{1,n}| \leq \frac{1}{\sqrt{\Delta x}} \|\eta_n\|_2, \quad |\psi_{1,n}| \leq \frac{1}{\sqrt{\Delta x}} \|\psi_n\|_2.$$

This would imply

$$\|\beta^{-n}\psi_1\|_{\ell^2(0,N)} \|\eta_1\|_{\ell^2(0,N)} \leq 2 \frac{\Delta t}{\Delta x} \|\psi_0\|_2^2 \sum_{n=0}^N \beta^{-2n} (1 + \beta_1^{2n}),$$

i.e.

$$\|\eta_{N+1}\|_2^2 \leq \frac{(1 + \beta)^2}{2\beta^2} \frac{\Delta t}{\Delta x} g_{0,J}^{\max} \|\psi_0\|_2^2 \sum_{n=0}^N \beta^{-2n} (1 + \beta_1^{2n}). \quad (6.37)$$

This yields finally the *error estimate*

$$\|\kappa_n\|_2^2 \leq g_{0,J}^{\max} \frac{\|\psi_0\|_2^2}{2\Delta x} \cdot \Delta t (1 + \beta)^2 \left[\frac{\beta^{2n} - 1}{\beta^2 - 1} + \frac{\beta^{2n} \beta_1^{2n}}{\beta^2 - \beta_1^2} \right]. \quad (6.38)$$

This estimate can be applied if we assume that $\Delta x = \text{const}$ (which corresponds to Case 2 of Section 5, cf. Theorem 5.1). The advantage of (6.38) is that the condition (6.14) is not necessary.

Note that $g_{0,J}^{\max}$ is the discrete analogue of $f_{0,X}^{\max}$ from (6.10). With the standard connection between Laplace– and Z –transforms we have:

$$\frac{\hat{g}_0^{\text{TBC}}(e^{s\Delta t}) - 1}{\Delta x} \rightarrow \hat{f}_0^{\text{TBC}}(s), \quad \Delta x, \Delta t \rightarrow 0,$$

$s = \alpha + i\xi$ fixed.

Example 6.5. (“cut-off” DTBC) We consider the simplified DTBC of Example 5.4 where the convolution coefficients $s_{j,n}$ are cut off for $n \geq N$. In Figure 11 we verify for $N = 10$ that the corresponding transformed convolution kernel (cf. (5.25)) satisfies the condition for the h^1 -a-priori estimate (6.14a) only for $\beta_2 \geq 1.24$.

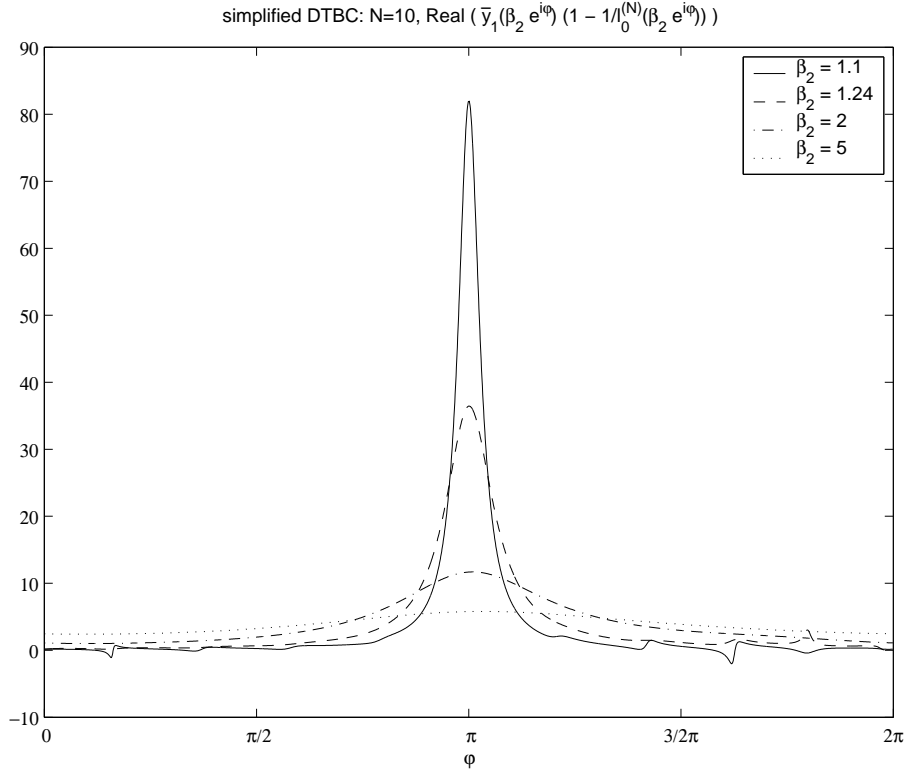


Figure 11: h^1 -condition (6.14a) for simplified discrete transparent boundary conditions with cut-off after $N = 10$ convolution coefficients, $\Delta x = 1/160$, $\Delta t = 2 \cdot 10^{-5}$, $V \equiv 0$. The h^1 -condition (6.14a) is satisfied for $\beta_2 \geq 1.24$.

As a discrete analogue of Example 6.2 we shall now illustrate the error estimate of Theorem 6.2: In (6.28) the error between the two solutions is

bounded by

$$\left\| \frac{1}{\hat{\ell}_j^{(N)}(\beta e^{i\varphi})} - \frac{1}{\hat{\ell}_j(\beta e^{i\varphi})} \right\|_{L^\infty(0,2\pi)}, \quad j = 0, J, \quad (6.39)$$

the difference between the exact $(\{\ell_{j,n}\})$ and the “cut-off” convolution kernels $(\{\ell_{j,n}^{(N)}\})$.

In the following table we show, how this difference (6.39) decreases as N , the number of retained convolution coefficients, grows. Theorem 6.2 hence implies convergence (as $N \rightarrow \infty$) of the corresponding discrete Schrödinger solutions for the scheme (5.10). The parameters are again $\Delta x = 1/160$, $\Delta t = 2 \cdot 10^{-5}$, $V \equiv 0$, and $\beta = 1.25$.

$N =$	5	10	20	30	40
error $\ 1/\hat{\ell}_0^{(N)} - 1/\hat{\ell}_0\ _\infty$	1.7346	0.97592	0.04391	0.004559	0.00048768

7 Numerical examples

In this section we shall present two examples to compare the numerical results from using our new approach of the approximated DTBC with the sum-of-exponentials-ansatz (3.1) (with $\nu = 2$) to the solution using the exact DTBC (1.16).

Example 7.1. *As a first example we consider the Schrödinger equation (1.1) in one space dimension on $0 \leq x \leq 1$ with $V \equiv 0$, and initial data $\psi^I(x) = \exp(i100x - 30(x - 0.5)^2)$. The time evolution of the approximate solution $|\psi_a(x, t)|$ using the approximated DTBC with convolution coefficients $\{\tilde{s}_n\}$ and $L = 10$, $L = 20$ is shown, respectively, in Figure 12 and Figure 13 (observe the viewing angle).*

While one can observe some reflected wave when using the approximated DTBC with $L = 10$, there are no reflections visible when using the approximated DTBC with $L = 20$.

Next we investigate the long-time stability behaviour of the approximated DTBC with the sum-of-exponentials ansatz. The reference solution ψ_{ref} with $\Delta x = 1/160$, $\Delta t = 2 \cdot 10^{-5}$ is obtained by using exact DTBCs (1.16) at the end points $x = 0$ and $x = 1$. We vary the parameter $L = 20, 30, 40, 50$ in (3.1) to find the corresponding approximate DTBCs, and show the error of the

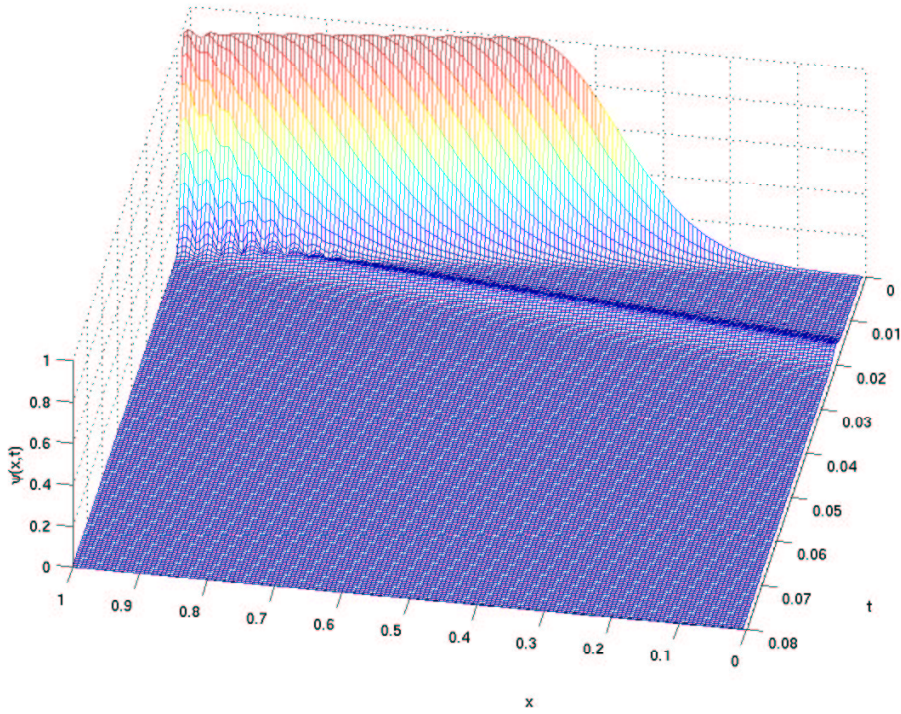


Figure 12: Time evolution of $|\psi_a(x, t)|$: The approximate convolution coefficients consisting of $L = 10$ discrete exponentials give rise to a reflected wave.

approximate solution ψ_a measured in $\|\psi_a(t) - \psi_{ref}(t)\|_{L_2} / \|\psi^I\|_{L_2}$. The result up to time step $n = 15000$ is shown in the Figure 14(a). Larger values of L clearly yield more accurate coefficients and hence a more accurate solution ψ_a .

In Figure 14(b) we show the analogous result for the “cut-off” DTBC, where we retained $N = 20, 30, 40, 50$ exact convolution coefficients. While the numerical effort is the same for both approaches with $L = N$, our sum-of-exponentials DTBC yields an error that is 3-4 orders of magnitude smaller.

Example 7.2. The second example considers the time evolution of a wave function in a potential well of finite depth: We solve the 1D-Schrödinger equation (1.1) on $[0, 2]$ with zero potential in the interior ($V(x) \equiv 0$ for $0 <$

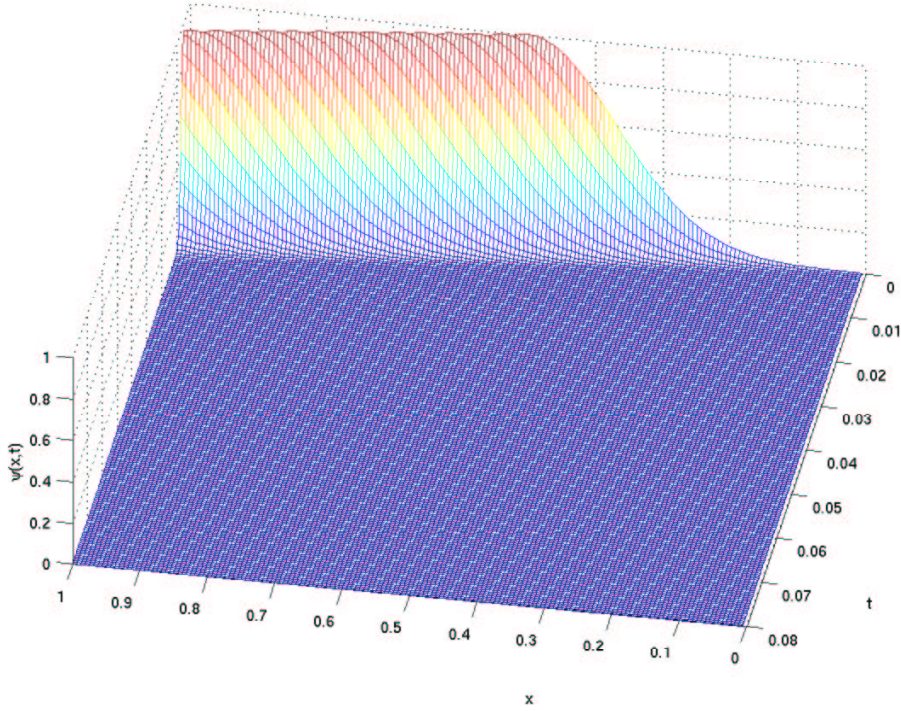


Figure 13: Time evolution of $|\psi_a(x, t)|$: The approximate convolution coefficients consisting of $L = 20$ discrete exponentials make reflections already invisible.

$x < 2$) and $V(x) \equiv 4500$ outside the computational domain. Figure 15 shows the time evolution of a right travelling Gaussian beam $[\psi^I(x) = \exp(i100x - 30(x-1)^2)]$ using the rather coarse space discretization $\Delta x = 1/160$, the time step $\Delta t = 2 \cdot 10^{-5}$, and the exact DTBC (1.16). We observe in Figure 15 that the main part of the wave is reflected at the boundaries. The value of the potential is chosen such that at time $t = 0.08$, i.e. after 4000 time steps 75% of the mass ($\|\psi(\cdot, t)\|_2^2$) has left the domain.

While the discrete TBCs (1.16) yield the exact numerical solution to the discrete whole-space problem (up to round-off errors), the approximated DTBC induces small errors. Figure 16 shows the error of the approximate solution ψ_a defined by $e_L(x, t) := (\psi_a(x, t) - \psi_{ref}(x, t)) / \|\psi^I\|_{L_2}$.

Figure 17 shows the time decay of the discrete ℓ^2 -norm $\|\psi(\cdot, t)\|_2$ and the temporal evolution of the error $\|e_L(\cdot, t)\|_2$ when using an approximated

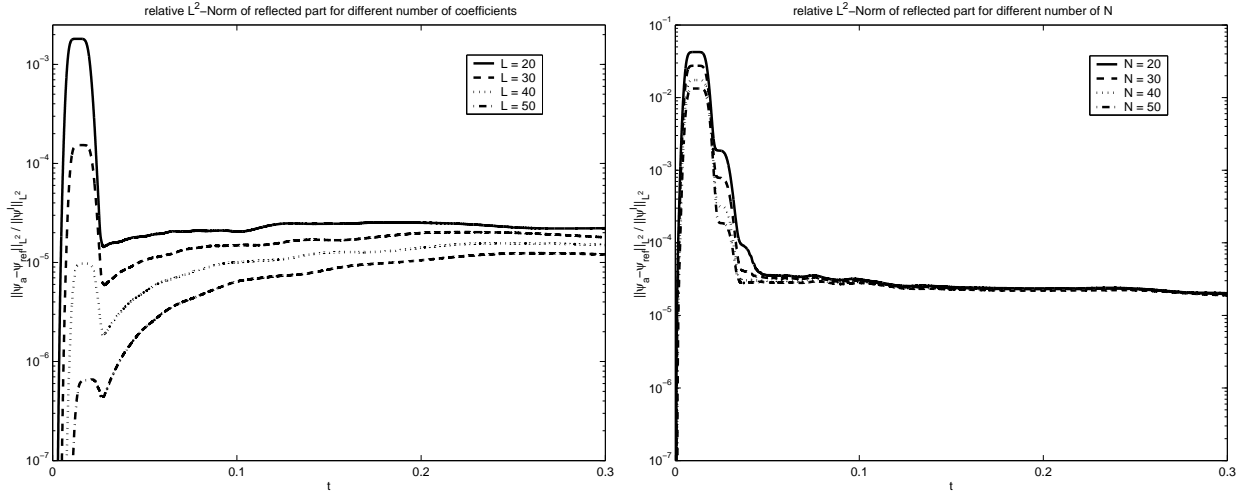


Figure 14: Error of the approximate solution $\psi_a(t)$ with (a) approximate convolution coefficients consisting of $L = 20, 30, 40, 50$ discrete exponentials; (b) “cut-off” DTBC: The convolution coefficients are cut off for $n \geq N$ with $N = 20, 30, 40, 50$. The error-peak between $t = 0.01$ and $t = 0.02$ corresponds to the first reflected wave, which is clearly visible in Figure 12.

DTBC with $L = 20, 30, 40$. Additionally, we calculated for $L = 20$ the coefficients $\{b_l, q_l\}$ for the “normalized parameters” $\Delta x = 1, \Delta t = 1, V = 0$ (cf. Appendix A) and then used the Transformation rule 3.1 to calculate the coefficients $\{b_l^, q_l^*\}$ for the desired parameters (cf. Example 3.1). The result is better than calculating the convolution coefficients “directly” (compare the error-curves “ $L = 20$ (trafo)” and “ $L = 20$ ”). One observes that the error increases with time. This is not surprising since each reflection at the boundaries induces an additional error.*

Evaluating the convolution appearing in exact DTBCs is quite expensive for long-time calculations. Therefore we shall now illustrate the difference in the computational effort for both approaches in Figure 18: The computational effort for the exact DTBCs is quadratic in time, since the evaluation of the boundary convolutions dominates for large times. On the other hand, the effort for the approximated DTBC only increases linearly. For $L = 10, 20, 30$ the lines are indistinguishable since the evaluation of the sum-of-exponential convolutions has a negligible effort compared to solving the PDE in the inte-

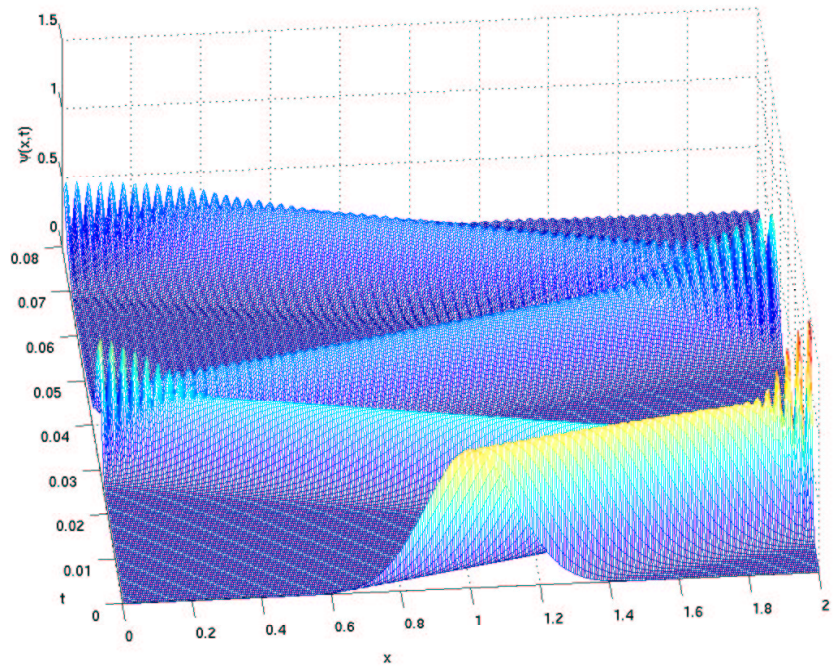


Figure 15: Time evolution of $|\psi(x,t)|$ in a potential well. The Gaussian beam is almost perfectly reflected by the walls of height $V = 4500$.

rior domain.

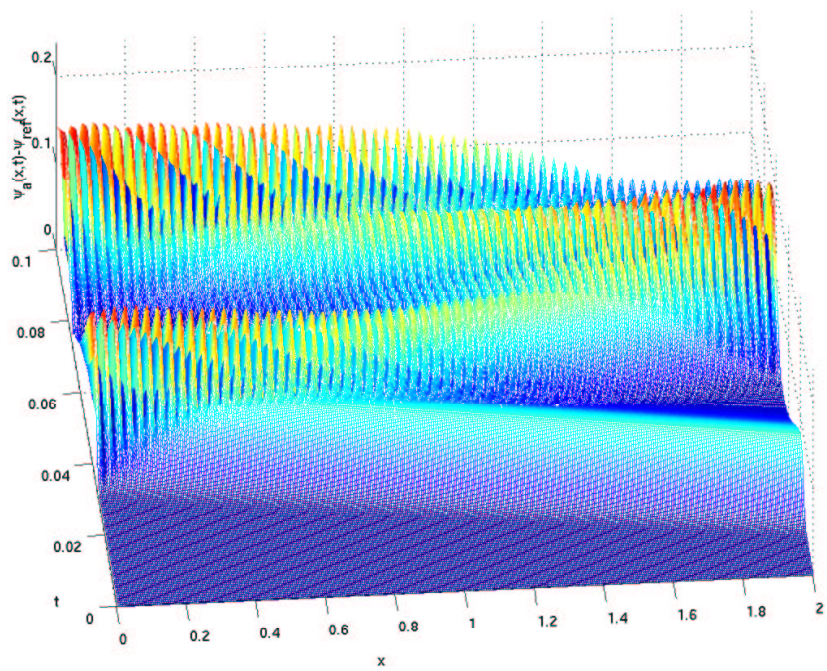


Figure 16: Time evolution within the potential well ($V = 4500$) of the error $|e_L(x, t)|$ due to an approximated DTBC with $L = 20$. As expected, the error accumulates with each reflection of the main wave.

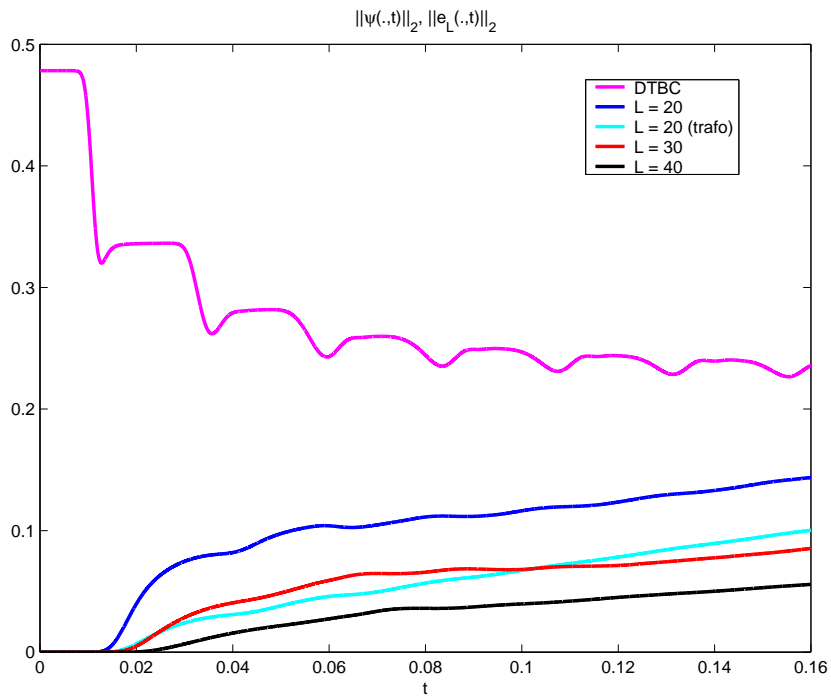


Figure 17: Time evolution within the potential well ($V = 4500$) of the discrete ℓ^2 -norm $\|\psi(\cdot, t)\|_2$ and of the errors $\|e_L(\cdot, t)\|_2$ that are due to approximated DTBCs with $L = 20, 30, 40$. “ $L = 20$ (trafo)” uses convolution coefficients calculated by the Transformation 3.1.

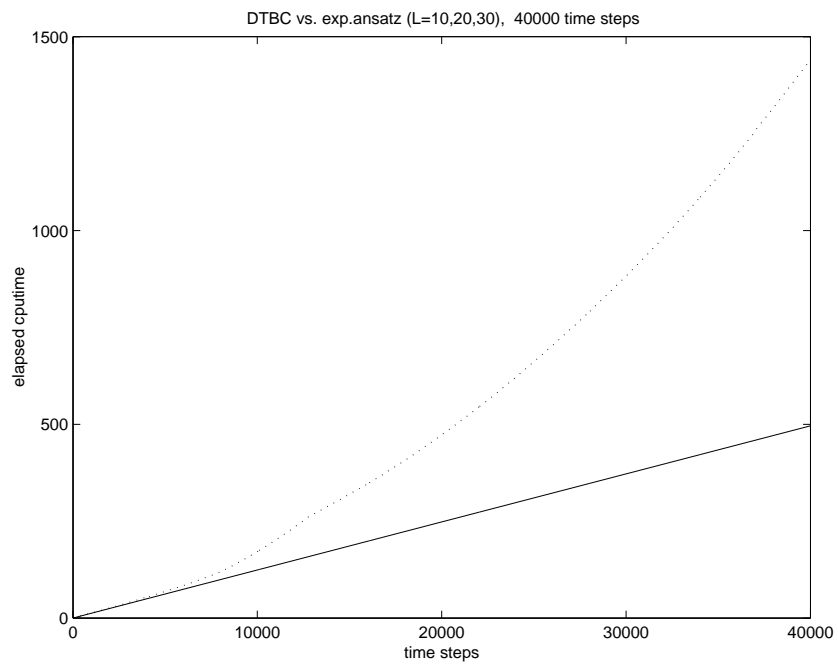


Figure 18: Comparison of CPU times: the sum-of-exponential approximation to DTBCs has linear effort (—), while exact DTBCs have quadratic effort.

Appendix A

In the following table we list the coefficients $\{q_l, b_l\}$ of the exponential-sums-BC having the convolution kernel (3.1) for the cases $L = 5$, and $L = 10$ with the “normalized parameters” $\nu = 2$, $\Delta x = \Delta t = 1$, and $V = 0$:

	q_l	b_l
L=5	$1.0613253 + 0.83506991e-1*I$	$-0.46123493e-1 - 0.35384269e-1*I$
	$0.83506991e-1 + 1.0613253*I$	$0.57634691e-1 + 0.75937784e-2*I$
	$1.1653982 + 0.41107342*I$	$-0.95195640e-1 - 0.20683503*I$
	$0.41107342 + 1.1653982*I$	$0.21356793 - 0.78940966e-1*I$
	$0.95734921 + 0.95734921*I$	$0.13684972 - 0.33038444*I$
L=10	$1.0204790 + 0.20818849e-1*I$	$-0.81657939e-2 - 0.36037147e-2*I$
	$0.20818849e-1 + 1.0204790*I$	$0.83222994e-2 + 0.32258771e-2*I$
	$1.0793585 + 0.91985074e-1*I$	$-0.31636868e-1 - 0.19266238e-1*I$
	$0.91985074e-1 + 1.0793585*I$	$0.35993931e-1 + 0.87473565e-2*I$
	$1.1613828 + 0.24003468*I$	$-0.61222441e-1 - 0.61543495e-1*I$
	$0.24003468 + 1.1613828*I$	$0.86808626e-1 - 0.22701935e-3*I$
	$1.2133719 + 0.49825873*I$	$-0.60889615e-1 - 0.14138908*I$
	$0.49825873 + 1.2133719*I$	$0.14303264 - 0.56921716e-1*I$
	$1.1272018 + 0.84466563*I$	$0.22117261e-1 - 0.20911201*I$
$0.84466563 + 1.1272018*I$	$0.13222525 - 0.16350378*I$	

The coefficients b_l^*, q_l^* for other parameters $\Delta x_*, \Delta t_*, V_*$ can then be obtained from the explicit formulas in the Transformation rule 3.1. A Java-Applet for calculating b_l^*, q_l^* is available on the authors' homepages: www.math.uni-muenster.de/u/arnold/dtbc.html, www.math.tu-berlin.de/~ehrhardt/

Appendix B

Here we present the Maple code that was used to calculate the coefficients q_l, b_l in the approximation (3.1) including the explicit formulas in Transformation rule 3.1. These codes can also be downloaded from the authors' homepages.

1. Parameters:

```
> restart;
> nu:=2; # initial index of approximation, cf. (3.1)
> L:=20; # number of terms in the sum of exponentials
> nc:=2*L-1; # number of convolution coefficients
> filename:="coe_L20V0";
> filenameetrafo:="coetrafo_L20V4500";
```

Parameters of the scheme:

```
> hp:=1; # scaled Planck constant
> Vr:=0.0; # potential in exterior domain  $x>=X$ 
> dx:=1.0; dt:=1.0;
> nco:=nc+nu; Digits1:=nco; Digits:=Digits1;
> rr:=4*dx^2/(dt*hp); # 'R' cf. (1.8)
> sig:=2*dx^2*Vr/hp^2; # parameters (1.17)
> fij:=arctan(2*rr*(sig+2)/(rr^2-4*sig-sig^2));
> efi:=exp(-I*fij);
> alj:=I/2*root[4]((rr^2+sig^2)*(rr^2+(sig+4)^2))*exp(I*fij/2);
```

2. Numerical inverse Z-transformation of the given analytical kernel (\hat{s})

The function ' \hat{s} ', see (1.11), (1.13), is considered outside the unit circle.

```
> lcoe:=proc(n,mm)
> # 'n' is No. of Fourier coef.
> # 'mm' is the number of grid intervals
> local ss, x, x1, x2, i, hat_s, shift;
> shift:=evalf(1.0); ss:=0;
> for i from 1 to mm do
>   x:=2*Pi*I*i/mm; x1:=exp(x+shift);
>   # calculation hat_s, cf. (1.11)&(1.13)
>   hat_s:=evalf((x1+1)/x1*subs(x2=rr/2*(x1-1)/(x1+1)+
>     I*dx^2*Vr,1-I*x2-I*sqrt(x2*(2*I+x2))));
>   ss:=ss+evalf(exp(n*x))*hat_s
> od;
> ss/mm*evalf(exp(n*shift)) end; # cf. (2.2)
```

Calculation of the convolution coefficients:

```
> mm:=nco+1;
> Digits:=Digits1: a1:=lcoe(nco,mm);
> # Checking the accuracy (last coefficient)
> Digits:=2*Digits1: a2:=lcoe(nco,2*mm);
> Digits:=Digits1: abs(a1-a2);
> mm:=nco+1;
```

```

> # Convolution coefficients:
> for i from 0 to nco do
>   coefc[i]:=lcoe(i,mm); # cf. (2.2)
> od;
> coefr[0]:=coefc[0]; coefr[1]:=coefc[1];
> # Extraction of the real part from s_n, n>1, cf. (1.18)
> for i from 2 to nco do
>   coefr[i]:=coefc[i]/exp(-I*i*fij)/alj;
>   coef[i]:=Re(coefr[i]);
> od;

```

3. Approximation

Calculation of the polynomial 'sp'. Only the coefficients starting with n=nu are used here; i.e. coef[0], coef[1], ..., coef[nu-1] are not considered.

```

> for i from 0 to nco-nu do
>   ac[i]:=coef[i+nu]:
> od:
> with(powseries):
> powcreate(e(n4)=ac[n4]):
> s1:=tpsform(e, x, nco-nu+1):
> sp:=sort(convert(s1,polynom));

```

Calculation of a rational function approximating the polynomial 'sp'. This is the usual Padé algorithm. The parameter 'npow' defines the orders of the numerator and denominator. Important: We have to check that the roots of the denominator are larger than 1 in absolute value. The value of 'npow' influences this property: Cycle A automatically chooses smaller and smaller values of 'npow' (L-1, L-2, ...) to guarantee that all roots have an absolute value larger than 1.

```

> nge1:=1; dnpow:=0; npow:=L;
> for ige1 from 1 by 1 while nge1 > 0 do
>   # cycle A
>   Digits:=8*nco; npow:=npow-dnpow;
>   with(numapprox): sr1:=pade(sp,x,[npow-1,npow]);
>   Digits:=Digits1: sr:=evalf(normal(sr1)):
>   pk:=sort(numer(sr)):
>   qk:=sort(denom(sr)):
>   roots1:=fsolve(qk,x,complex):
>   nroffroots:= 0:
>   for r in roots1 do
>     nroffroots:=nroffroots+1;
>   od:

```

```

> nroffroots;
> nge1:=0:
> for i from 1 to nroffroots do
>   if (evalf(abs(roots1[i]))<1) then nge1:=nge1+1 fi:
>   dnpow:=nge1:
>   appendto(terminal);
> od;
> lprint(nge1);
> # ---> number of roots with abs < 1
> appendto(terminal);
> od:
> # printing of roots
> for i from 1 to nroffroots do
>   lprint(evalf(abs(roots1[i])));
>   appendto(terminal);
> od;

```

Writing of the result:

```

> for i from 1 to nroffroots do
>   Digits:=Digits1:
>   # Coming back to complex q_l (factor exp(I*fij))
>   q[i]:=roots1[i]*exp(I*fij);
>   # Coming back to complex b_l (factor alj/exp(I*(nu-1)*fij))
>   be[i]:=-subs(x=roots1[i],pk)/subs(x=roots1[i],diff(qk,x))
>     *(alj/exp(I*(nu-1)*fij))*q[i]^(nu-1):
>   qRef:=Re(q[i]): qImf:=Im(q[i]):
>   bRef:=Re(be[i]): bImf:=Im(be[i]):
>   Digits:=14:
>   appendto(filename):
>   lprint(evalf(qRef),evalf(qImf),evalf(bRef),evalf(bImf)):
>   appendto(terminal):
> od:

```

Checking of our representation:

```

Digits:=Digits1:
L:=nroffroots:
ap:=proc(n)
local ss, i; ss:=0;
for i from 1 to L do
  ss:=ss+be[i]*q[i]^(-n) # cf. (3.1)
od;
ss end;

```

First nco coefficients:

```

appendto(terminal);
for i from nu to nc+nu do apc[i]:= ap(i): od:
for i from nu to nc+nu do i:
  coefc[i]; eps:=abs(apc[i]-coefc[i]);
od;

```

4. Transformation to other grid parameters, see Transformation 3.1

```

> Vrs:=4500; dxs:=1/160; dts:=0.00002;
> a:=2*dx^2/dt+2*dxs^2/dts+I*(dx^2*Vr-dxs^2*Vrs); # (3.15)
> b:=2*dx^2/dt-2*dxs^2/dts-I*(dx^2*Vr-dxs^2*Vrs); # (3.16)
> for i from 1 to L do
>   qs[i]:=(q[i]*conjugate(a)-conjugate(b))/
>     (a-q[i]*b): # (3.13)
> od;
> for i from 1 to L do
>   bes[i]:=be[i]*q[i]*((a*conjugate(a)-b*conjugate(b))/
>     ((a-q[i]*b)*(q[i]*conjugate(a)-conjugate(b))))*
>     (1+qs[i])/(1+q[i]): # (3.14)
>   qsRef:=Re(qs[i]): qsImf:=Im(qs[i]):
>   bsRef:=Re(bes[i]): bsImf:=Im(bes[i]):
>   Digits:=14:
>   appendto(filenameetrafo):
>   lprint(evalf(qsRef),evalf(qsImf),evalf(bsRef),evalf(bsImf)):
>   appendto(terminal):
> od;
> L:=nrofroots; # (3.1)
> aps:=proc(n)
> local ss, i; ss:=0;
> for i from 1 to L do
>   ss:=ss+bes[i]*qs[i]^(-n)
> od;
> ss end;

```

First nco new convolution coefficients (starting with n=nu):

```

> appendto(terminal);
> for n from nu to nc+nu do apcs[n]:= aps(n): od:
> for n from nu to nc+nu do coefs[n]:= apcs[n]; od;

```

References

- [1] B. Alpert, L. Greengard and T. Hagstrom, *Rapid evaluation of nonreflecting boundary kernels for time-domain wave propagation*, SIAM J. Numer. Anal. **37** (2000), 1138–1164.
- [2] B. Alpert, L. Greengard and T. Hagstrom, *Nonreflecting Boundary Conditions for the Time-Dependent Wave Equation*, J. Comp. Phys. **180** (2002), 270–296.
- [3] I. Alonso-Mallo and N. Reguera, *Weak ill-posedness of spatial discretizations of absorbing boundary conditions for Schrödinger-type equations*, SIAM J. Numer. Anal. **40** (2002), 134–158.
- [4] A. Arnold, *Numerically Absorbing Boundary Conditions for Quantum Evolution Equations*, VLSI Design **6** (1998), 313–319.
- [5] A. Arnold and M. Ehrhardt, *Discrete transparent boundary conditions for wide angle parabolic equations in underwater acoustics*, J. Comp. Phys. **145** (1998), 611–638.
- [6] A. Arnold, *Mathematical concepts of open quantum boundary conditions*, Transp. Theory Stat. Phys. **30**, 4-6 (2001), 561–584.
- [7] G.A. Baker, Jr., *Essentials of Padé Approximants*, Academic Press NY, San Francisco, London, 1975.
- [8] V.A. Baskakov and A.V. Popov, *Implementation of transparent boundaries for numerical solution of the Schrödinger equation*, Wave Motion **14** (1991), 123–128.
- [9] N. Ben Abdallah, *On a multi-dimensional Schrödinger-Poisson Scattering model for semiconductors*, J. Math. Phys. **41**, 7 (2000), 2241–2261.
- [10] C.H. Bruneau and L. Di Menza, *Conditions aux limites transparentes et artificielles pour l'équation de Schrödinger en dimension 1 d'espace*, C. R. Acad. Sci. Paris, Ser. I **320** (1995), 89–94.
- [11] L. Burgnies, O. Vanbésien and D. Lippens, *Transient analysis of ballistic transport in stublike quantum waveguides*, Appl. Phys. Lett. **71**, 6 (1997), 803–805.
- [12] R. Dautray and J.L. Lions, *Mathematical Analysis and Numerical Methods for Science and Technology*, Vol. 5—Evolution Problems I, Springer, Berlin, 1992.

- [13] A. Dedner, D. Kröner, I. Sofronov and M. Wesenberg, *Transparent Boundary Conditions for MHD Simulations in Stratified Atmospheres*, J. Comp. Phys. **171** (2001), 448–478.
- [14] L. Di Menza, *Approximations numériques d'équations de Schrödinger non linéaires et de modèles associés*, Ph.D. thesis, Université Bordeaux I, 1995.
- [15] G. Doetsch, *Anleitung zum praktischen Gebrauch der Laplace-Transformation und der Z-Transformation*, R. Oldenburg Verlag München, Wien, 3. Auflage 1967.
- [16] M. Ehrhardt, *Discrete Transparent Boundary Conditions for Parabolic Equations*, Z. Angew. Math. Mech. **77** (1997) S2, 543–544.
- [17] M. Ehrhardt and A. Arnold, *Discrete Transparent Boundary Conditions for the Schrödinger Equation*, Rivista di Matematica della Università di Parma **6** (2001), 57–108.
- [18] M.J. Grote and J.B. Keller, *Exact nonreflecting boundary conditions for the time dependent wave equation*, SIAM J. Appl. Math. **55** (1995), 280–297.
- [19] T. Hagstrom, *Radiation boundary conditions for the numerical simulation of waves*, Acta Numerica **8** (1999), 47–106.
- [20] J.R. Hellums and W.R. Frensley, *Non-Markovian open-system boundary conditions for the time-dependent Schrödinger equation*, Phys. Rev. B **49** (1994), 2904–2906.
- [21] M.A. Lavrent'ev and B.V. Shabat, *Methods for the theory of functions of a complex variable*, 5th rev. ed., (Russian), Moskva: Nauka, 1987.
- [22] M.F. Levy, *Non-local boundary conditions for radiowave propagation*, in: Third International Conference on Mathematical and Numerical Aspects of Wave Propagation Phenomena, Juan-les-Pins, France, 24-28 April 1995.
- [23] C. Lubich, *Convolution Quadrature and Discretized Operational Calculus. I*, Numer. Math. **52** (1988), 129–145.
- [24] C. Lubich, *Convolution Quadrature and Discretized Operational Calculus. II*, Numer. Math. **52** (1988), 413–425.
- [25] C. Lubich, *On the multistep time discretization of linear initial-boundary value problems and their boundary integral equations*, Numer. Math. **67** (1994), 365–389.

- [26] C. Lubich and A. Schädle, *Fast convolution for non-reflecting boundary conditions*, SIAM J. Sci. Comput. **24** (2002), 161–182.
- [27] J.N. Lyness and G. Sande, *Algorithm 413: ENTCAF and ENTCRE: Evaluation of Normalized Taylor Coefficients of an Analytic Function*, Comm. ACM **14** (1971), 669–675.
- [28] B. Mayfield, *Non-local boundary conditions for the Schrödinger equation*, Ph.D. thesis, University of Rhode Island, Providence, RI, 1989.
- [29] K.B. Oldham and J. Spanier, *The Fractional Calculus - Differentiation and Integration to Arbitrary Order*, Academic Press, Boston, 1974.
- [30] J.S. Papadakis, *Impedance formulation of the bottom boundary condition for the parabolic equation model in underwater acoustics*, NORDA Parabolic Equation Workshop, NORDA Tech. Note 143, 1982.
- [31] A. Quarteroni and A. Valli, *Numerical approximation of partial differential equations*, Springer, Berlin, 1994.
- [32] V.S. Ryaben’kii, *Exact Transfer of Difference Boundary Conditions*, Functional Anal. Appl. **24** (1990), 251–253.
- [33] V.S. Ryaben’kii, *Exact transfer of boundary conditions*, Comput. Mech. of Solids **1** (1990), 129–145 (in Russian).
- [34] A. Schädle, *Numerische Behandlung transparenter Randbedingungen für die Schrödinger-Gleichung*, Masters Thesis, Universität Tübingen, 1998.
- [35] A. Schädle, *Non-reflecting boundary conditions for the two dimensional Schrödinger equation*, Wave Motion **35** (2002), 181–188.
- [36] A. Schädle, *Ein schneller Faltungsalgorithmus für nichtreflektierende Randbedingungen*, Ph.D. Thesis, Universität Tübingen, 2002.
- [37] F. Schmidt and P. Deuffhard, *Discrete transparent boundary conditions for the numerical solution of Fresnel’s equation*, Comput. Math. Appl. **29** (1995), 53–76.
- [38] F. Schmidt and D. Yevick, *Discrete transparent boundary conditions for Schrödinger-type equations*, J. Comp. Phys. **134** (1997), 96–107.
- [39] F. Schmidt, *Construction of discrete transparent boundary conditions for Schrödinger-type equations*, Surv. Math. Ind. **9** (1999), 87–100.
- [40] I.L. Sofronov, *Conditions for Complete Transparency on the Sphere for the Three-Dimensional Wave Equation*, Russian Acad. Sci. Dokl. Math. **46** (1993), 397–401.

- [41] I.L. Sofronov, *Artificial Boundary Conditions of Absolute Transparency for Two- and Threedimensional External Time-Dependent Scattering Problems*, Euro. J. Appl. Math. **9** (1998), 561–588.
- [42] I.L. Sofronov, *Non-reflecting inflow and outflow in wind tunnel for transonic time-accurate simulation*, J. Math. Anal. Appl. **221** (1998), 92–115.
- [43] L. Ting and M.J. Miksis, *Exact Boundary Conditions for Scattering Problems*, J. Acoust. Soc. Am. **80** (1986), 1825–1827.
- [44] F.D. Tappert, *The parabolic approximation method*, in *Wave Propagation and Underwater Acoustics*, Lecture Notes in Physics 70, eds. J.B. Keller and J.S. Papadakis, Springer, New York, 1977, pp. 224–287.
- [45] A. Zisowsky, *Discrete Transparent Boundary Conditions for Parabolic Systems*, Preprint (2002).